Dicer-2-Dependent Generation of Viral DNA from Defective Genomes of RNA Viruses Modulates Antiviral Immunity in Insects

Enzo Poirier, Bertsy Goic, Lorena Tomé-Poderti, Lionel Frangeul, Jeremy Boussier, Valérie Gausson, Hervé Blanc, Thomas Vallet, Hyelee Loyd, Laura Levi, et al.

Article

Cell Host & Microbe

Dicer-2-Dependent Generation of Viral DNA from Defective Genomes of RNA Viruses Modulates Antiviral Immunity in Insects

Graphical Abstract

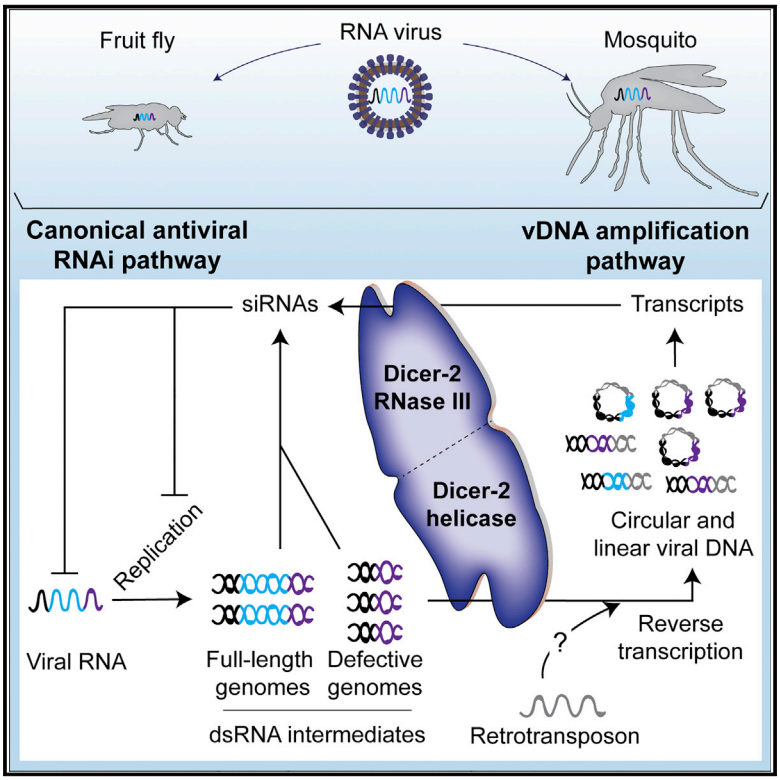

Highlights

- Circular viral DNAs (vDNAs) produced during RNA virus infection are a source of siRNAs
- Defective viral genomes (DVG) serve as templates for vDNA synthesis
- The helicase domain of Dicer-2 modulates vDNA production and virus persistence
- DVGs serve to amplify siRNA-mediated antiviral immunity in insects

Authors

Enzo Z. Poirier, Bertsy Goic, Lorena Tomé-Poderti, ..., Susan Carpenter, Marco Vignuzzi, Maria-Carla Saleh

Correspondence

marco.vignuzzi@pasteur.fr (M.V.), carla.saleh@pasteur.fr (M.-C.S.)

In Brief

Poirier et al. show that during RNA virus infection of insects, circular viral DNA is produced, regulated by Dicer-2 helicase domain. The main template for viral DNA is defective viral genomes, which appear to be key viral products modulating the host immune response and the establishment of viral persistence.

Poirier et al., 2018, Cell Host & Microbe *23*, 353–365
March 14, 2018
https://doi.org/10.1016/j.chom.2018.02.001

CellPress

Cell Host & Microbe
Article

Dicer-2-Dependent Generation of Viral DNA from Defective Genomes of RNA Viruses Modulates Antiviral Immunity in Insects

Enzo Z. Poirier,[1,2,3] Bertsy Goic,[1] Lorena Tomé-Poderti,[1,8] Lionel Frangeul,[1,8] Jérémy Boussier,[4] Valérie Gausson,[1] Hervé Blanc,[1,2] Thomas Vallet,[2] Hyelee Loyd,[5] Laura I. Levi,[2] Sophie Lanciano,[6] Chloé Baron,[1] Sarah H. Merkling,[7] Louis Lambrechts,[7] Marie Mirouze,[6] Susan Carpenter,[5] Marco Vignuzzi,[2,*] and Maria-Carla Saleh[1,9,*]

[1]Institut Pasteur, Viruses and RNA Interference, Centre National de la Recherche Scientifique UMR 3569, 75015 Paris, France
[2]Institut Pasteur, Viral Populations and Pathogenesis, Centre National de la Recherche Scientifique UMR 3569, 75015 Paris, France
[3]University of Paris Diderot, Sorbonne Paris Cité, Cellule Pasteur, 75013 Paris, France
[4]Institut Pasteur, Immunobiology of Dendritic Cells, Institut National de la Santé et de la Recherche Médicale, U1223, 75015 Paris, France
[5]Department of Animal Science, Iowa State University, Ames, IA 50010, USA
[6]Institut de Recherche pour le Développement, DIADE, Université de Montpellier, Université de Perpignan, LGDP, 66860 Perpignan, France
[7]Institut Pasteur, Insect-Virus Interactions, Centre National de la Recherche Scientifique URA 3012, 75015 Paris, France
[8]These authors contributed equally
[9]Lead Contact
*Correspondence: marco.vignuzzi@pasteur.fr (M.V.), carla.saleh@pasteur.fr (M.-C.S.)
https://doi.org/10.1016/j.chom.2018.02.001

SUMMARY

The RNAi pathway confers antiviral immunity in insects. Virus-specific siRNA responses are amplified via the reverse transcription of viral RNA to viral DNA (vDNA). The nature, biogenesis, and regulation of vDNA are unclear. We find that vDNA produced during RNA virus infection of *Drosophila* and mosquitoes is present in both linear and circular forms. Circular vDNA (cvDNA) is sufficient to produce siRNAs that confer partially protective immunity when challenged with a cognate virus. cvDNAs bear homology to defective viral genomes (DVGs), and DVGs serve as templates for vDNA and cvDNA synthesis. Accordingly, DVGs promote the amplification of vDNA-mediated antiviral RNAi responses in infected *Drosophila*. Furthermore, vDNA synthesis is regulated by the DExD/H helicase domain of Dicer-2 in a mechanism distinct from its role in siRNA generation. We suggest that, analogous to mammalian RIG-I-like receptors, Dicer-2 functions like a pattern recognition receptor for DVGs to modulate antiviral immunity in insects.

INTRODUCTION

The RNA interference (RNAi) machinery acts as the major antiviral mechanism in insects (Galiana-Arnoux et al., 2006; Li et al., 2002; van Rij et al., 2006). Dicer-2 (Dcr-2) detects viral dsRNA, from replication intermediates or RNA secondary structures, and processes it to produce 21 nt-long small-interfering RNAs (siRNAs) that are subsequently loaded into a RNA-induced silencing complex (RISC). As part of the RISC complex, the Argonaute-2 (Ago2) endonuclease degrades cognate viral RNA in a sequence-specific manner (Liu et al., 2004). Recent studies (Goic et al., 2013, 2016) revealed a pathway for amplification of the virus-specific siRNA response in which viral RNA is reverse transcribed to viral DNA (vDNA) by cellular reverse transcriptase (RT) from long-terminal repeat (LTR) retrotransposons. Transcripts generated from vDNA feed into the RNAi machinery, resulting in more abundant and diverse siRNAs. Chemical inhibition of vDNA production by azidothymidine (AZT) treatment, in either *Drosophila* infected with flock house virus (FHV) or mosquitoes infected with chikungunya virus, leads to loss of virus persistence and death of infected animals (Goic et al., 2013, 2016). In addition, siRNAs transcribed from vDNA were shown to shuttle to uninfected cells via exosome transport and confer protection against infection (Tassetto et al., 2017). Thus, synthesis of vDNA is a component of the antiviral immune response in insects, pivotal to establishing persistent virus infections.

Although vDNA was shown to play a key role in antiviral immunity in insects, questions remain regarding the nature, biogenesis, and regulation of vDNA. The molecular events mediating initiation and extension of reverse transcription are well characterized for retroviruses and retrotransposons (Hughes, 2015); however, there is scant information on how viral RNA and retrotransposon RT interact to generate vDNA. The identification of retrotransposon-vDNA chimeras supports a model wherein vDNA arises through a copy-choice mechanism of recombination (Goic et al., 2013), which would require co-localization of viral RNA, RT, and retrotransposon RNA. Where this might occur is not apparent. During retrotransposition, reverse transcription occurs in the cytoplasm in virus-like particles (VLP) (Beauregard et al., 2008); thus viral RNA may be packaged into VLPs. In contrast, RNA virus replication occurs in membrane-associated replication complexes (Frolova et al., 2010; Grimley et al., 1972; Miller et al., 2001), and RT may localize to sites enriched in viral RNA/dsRNA. If so, a signaling mechanism activated during virus

infection may re-direct the RT complex toward replication sites or to the antiviral RNAi complex.

During RNA virus infection of mammals, pathogen-associated molecular patterns (PAMPs) are detected by cellular sensors named pattern recognition receptors (PRRs), which trigger type I interferon and other immune responses (Nan et al., 2014). One type of PRR, the cytoplasmic RIG-I-like receptors (RLRs), carries a DExD/H-box helicase domain that is phylogenetically related to the N-terminal DExD/H-box helicase domain of *Drosophila* Dcr-2 (Deddouche et al., 2008; Paro et al., 2015). Indeed, RLRs and *Drosophila* Dcr-2 are grouped into the duplex RNA-activated ATPases (DRAs) family (Luo et al., 2013). DRAs bind dsRNA and ATP, resulting in conformational changes that expose signaling domains and binding sites for partner proteins (Luo et al., 2013). The cytoplasmic RLRs preferentially bind short RNAs and defective viral genomes (DVGs), which comprise truncated or rearranged viral genomes and viral genomes carrying sequences of non-viral origin (Baum et al., 2010; Sanchez David et al., 2016; Marriott and Dimmock, 2010; Sun et al., 2015). DVGs are a byproduct of copy-choice recombination during viral replication, resulting from the high, yet relaxed, processivity of the viral RNA polymerase (Lazzarini et al., 1981; Simon-Loriere and Holmes, 2011). A sub-category of DVGs, referred to as defective interfering (DI) genomes, can inhibit productive virus replication by hijacking factors required for replication and packaging (Marriott and Dimmock, 2010). DVGs are produced by all arboviruses and can be transmitted between invertebrate and vertebrate hosts, as exemplified by the long-term transmission of a dengue virus DVG (Aaskov et al., 2006). In mammals, DVGs are known PAMPs that activate type I interferon through MAVS and participate in dendritic cell maturation (Yount et al., 2006, 2008). In *Drosophila*, DVGs are preferentially targeted by the RNAi machinery, suggesting a link between defective genomes and viral persistence (Jaworski and Routh, 2017; Jovel and Schneemann, 2011; Vodovar et al., 2011). The structural and functional similarities among RLRs, which sense DVGs in mammals, and other DRA family proteins raise the question of whether Dcr-2 plays a similar role in insects.

In this work, we dissect the nature, biogenesis, and mechanism of vDNA synthesis. We demonstrate that vDNA produced during infection of fruit flies and mosquitoes is present in both linear and circular form. The presence of circular viral DNA (cvDNA) per se is sufficient to produce siRNAs that confer partially protective immunity when challenged with a cognate virus. The sequences of cvDNAs bore homology to DVGs. We show that DVGs are a major template for vDNA and cvDNA synthesis in infected fruit flies and that they act as PAMPs in amplification of the vDNA-mediated antiviral RNAi response. Furthermore, we show that vDNA synthesis is regulated by the DExD/H helicase domain of Dcr-2 in a mechanism distinct from the generation of siRNAs. Together, these results suggest that Dcr-2 functions similar to a PRR, together with DVGs acting as PAMPs, to modulates the antiviral immune response in insects. Our work reveals a convergence between invertebrate antiviral immunity and the mammalian type I interferon response and suggests strategies to curtail arbovirus infections in insects by optimizing the protective response provided by circular viral DNAs.

RESULTS

Circular vDNA Produced during RNA Virus Infection of Insects Confers Virus-Specific Immunity

Elucidating mechanisms important in the biogenesis of vDNA may be gleaned from sequence analysis of vDNAs. The vDNA generated during FHV infection of *Drosophila* S2 cells and fruit flies is linked to LTR-retrotransposon sequences (Goic et al., 2013). Since most retrotransposons generate unintegrated circular DNA (Beauregard et al., 2008), we hypothesized that both circular and linear forms of vDNA would be present at early times after infection. Wild-type fruit flies were mock-infected or infected with FHV, *Drosophila* C virus (DCV), or Sindbis virus (Sindbis) and collected 7 (FHV and DCV) and 4 (Sindbis) days post-infection. A portion of total DNA was extracted and treated with DNase Plasmid-Safe, an ATP-dependent DNase that removes linear DNA. After treatment, DNA was analyzed by PCR using primers for viruses, mitochondrial DNA, and the Rp49 gene. Both mitochondrial (mtDNA) and Rp49 DNA were amplified in absence of DNase-PS (Figures 1A–1C). However, mtDNA, but not Rp49 DNA, was amplified in samples treated with DNase-PS, confirming that linear DNA was selectively removed by DNase-PS treatment (Figures 1A–1C). vDNA was present in both non-treated and DNase-PS-treated samples from FHV, DCV, and Sindbis-infected flies, but not in mock-infected flies (Tris). The amplification of viral sequences in DNase-PS-treated samples was confirmed by sequencing PCR products. Thus, both linear and circular viral DNA (cvDNA) were produced during infection in flies (Figures 1A–1C). Furthermore, cvDNA was detected as early as 16 hr after FHV infection (Figure S1A, related to Figure 1) and 24 hr after DCV infection (Figure S1B, related to Figure 1) in S2 *Drosophila* cells. Finally, we infected mosquitoes with chikungunya virus (CHIKV) and detected both linear and circular forms of CHIKV vDNA (Figure 1D). The presence of cvDNA in two different insects using four different viruses indicates that cvDNA is a common feature of the vDNA synthesis pathway during the antiviral immune response.

Since circular DNA is more stable than linear DNA, we examined the stability of vDNA produced in insect cells. For these experiments, we used a Sindbis replicon (Bredenbeek et al., 1993), which undergoes only a single replication cycle. Thus, any vDNA detected after infection was synthesized from this single cycle, allowing us to follow the fate of cvDNA molecules. Wild-type flies were infected with 1,000 particles of Sindbis-replicon and collected at various times post-inoculation (Figure 1E). cvDNA appeared as early as 24 hr post-infection and was maintained up to 2 weeks post-infection, indicating that cvDNA is an abundant and long-lasting form of vDNA.

The presence and persistence of cvDNA during infection in insects suggest that these circular forms are biologically relevant. Previous studies found that vDNA participates in the antiviral response (Goic et al., 2013, 2016; Tassetto et al., 2017), and we hypothesized that cvDNA may be sufficient to induce a protective, virus-specific immune response in naive flies. To test this, cvDNA (free of viral RNA) was isolated from FHV-infected *Drosophila* S2 cells (Figure S1C, related to Figure 1). Flies injected with this cvDNA were challenged with homologous FHV 2 days later. We observed a significant increase in survival time in flies immunized with cvDNA from FHV-infected

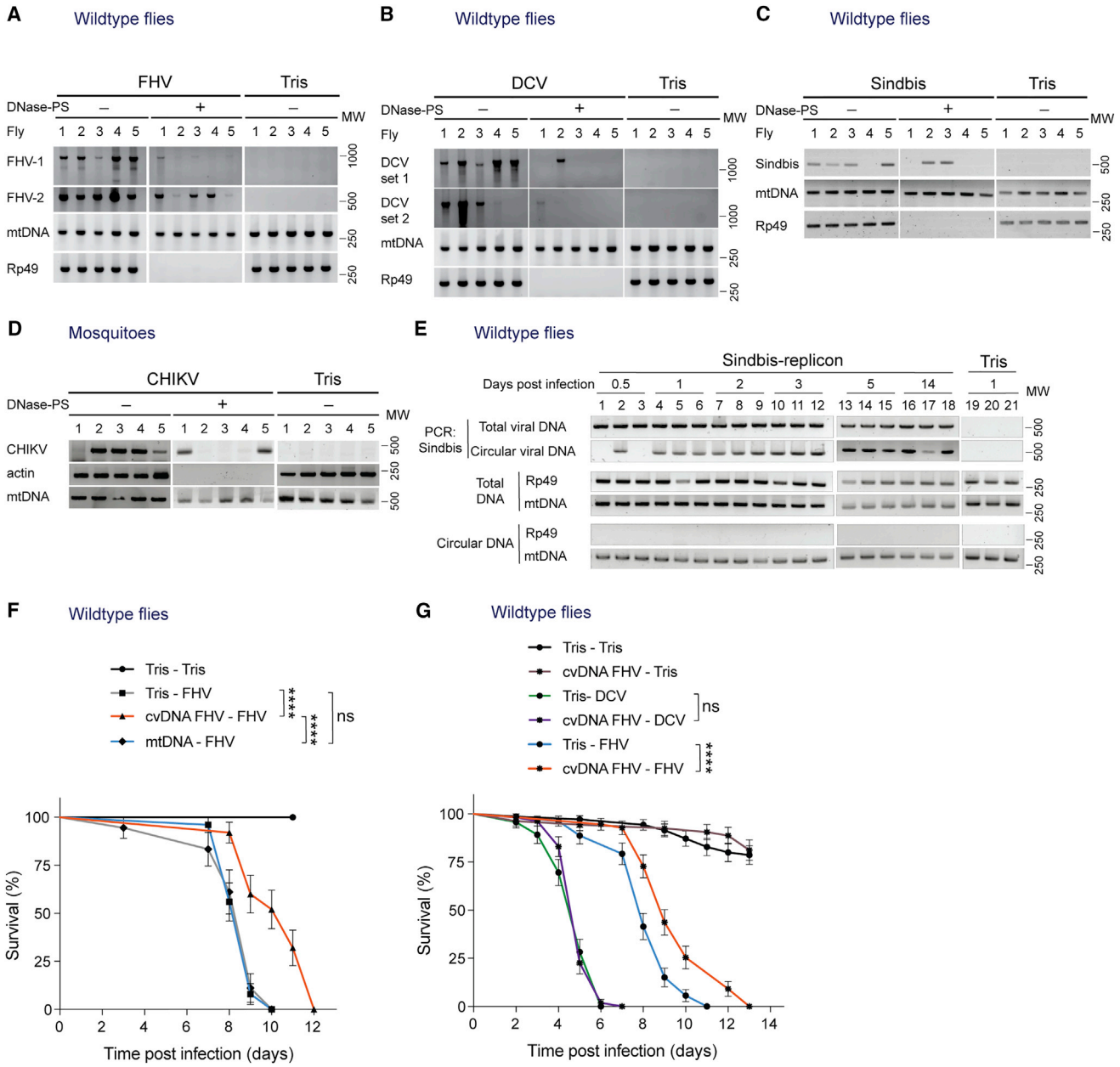

Figure 1. Circular vDNA Produced during RNA Virus Infection of Insects Confers Virus-Specific Protective Immunity

(A) Wild-type flies were infected with FHV or mock infected (Tris). DNA was extracted from individual flies and RNase treated, and linear DNA was digested with Plasmid-Safe DNase (DNase-PS). Amplification of Rp49 by PCR shows linear DNA, while amplification of mitochondrial DNA (mtDNA) is a control for circular DNA. Linear and circular DNA from FHV RNA1 and RNA2, the two FHV genomic segments, is detected by PCR.

(B) Flies were injected with DCV and processed as in (A).

(C) Flies were injected with Sindbis virus and processed as in (A).

(D) Mosquitoes were fed chikungunya virus (CHIKV) through a blood meal and processed as in (A). CHIKV circular vDNA presence was assessed by PCR, and actin was used as a control for linear DNA.

(E) Wild-type flies were infected with Sindbis replicon, and linear and circular forms of vDNA were detected as described in (A).

(F) Wild-type flies were immunized with 10 ng of circular vDNA isolated from FHV-infected S2 cells (cvDNA FHV), mitochondrial DNA isolated from uninfected S2 cells (mtDNA), or mock infected (Tris). Three days later, flies were challenged with 80 $TCID_{50}$ FHV or with Tris. "cvDNA FHV-FHV" indicates flies immunized with FHV cvDNA and challenged with FHV.

(G) Wild-type flies were immunized as described in (F) and challenged with 100 $TCID_{50}$ DCV or with 80 $TCID_{50}$ FHV. Survival was monitored daily. Molecular weights (MW) are indicated.

(A–G) Data are representative of three independent experiments. (F and G) Dots represent mean and SEM (n = 75 flies per condition). ns, not significant; ****$p < 0.0001$ (log-rank test). See also Figure S1.

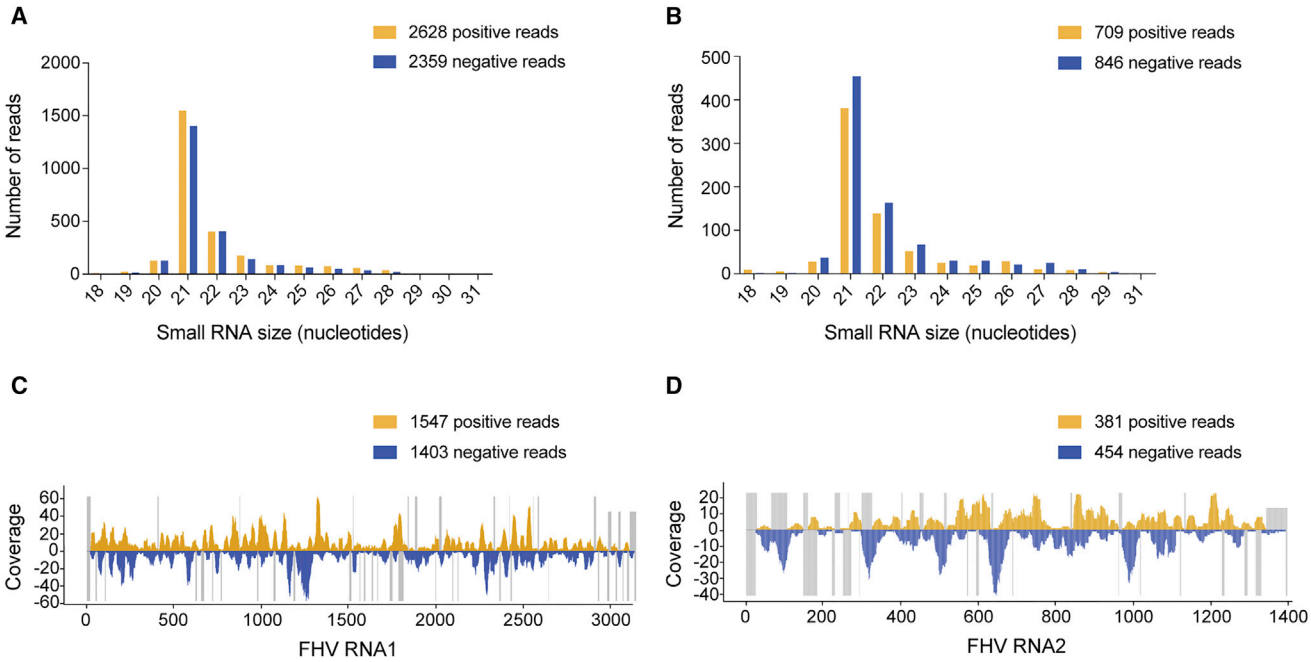

Figure 2. Circular vDNA Protection Is Mediated by the siRNA Response

(A and B) Circular vDNA isolated from FHV-infected S2 cells was injected into naive wild-type flies. siRNAs were deep sequenced at 3 days post-inoculation and mapped on FHV RNA1 and RNA2, respectively. Graph shows size distribution of small RNAs mapping on FHV genome.

(C and D) siRNA coverage from circular vDNA on FHV RNA1 and RNA2. Uncovered regions are represented as gray lines.

Data are representative of three independent experiments.

cells, but not circular DNA from uninfected cells (Figure 1F). This effect was sequence specific, as flies immunized with FHV cvDNA and challenged with DCV were not protected (Figure 1G). This increased survival was not accompanied by a similar decrease in virus titer (data not shown), as previously observed in mosquitoes (Goic et al., 2016). Together, these results demonstrate that a portion of vDNA produced during infection is circular, that the circular form is long lasting, and that cvDNA alone can induce a virus-specific immune response against homologous virus challenge.

Circular vDNA Protection Is Mediated by the siRNA Response

It is currently thought that vDNA amplifies the immune response by boosting production of siRNAs (Goic et al., 2013, 2016; Tassetto et al., 2017). To determine if cvDNA induces virus-specific siRNAs, we inoculated flies with cvDNA from FHV- and mock-infected S2 cells, and after 3 days small RNAs were purified and deep sequenced. We detected FHV RNA1- and RNA2-specific siRNAs of positive and negative polarity in flies injected with cvDNA from FHV-infected cells (Figures 2A and 2B), while no FHV-siRNAs were detected in flies injected with cvDNA from uninfected cells (data not shown). The siRNAs mapped across the FHV genome (Figures 2C and 2D), suggesting that cvDNAs comprise a large number of different viral sequences and/or full-length viral sequences. These data, together with results from the previous section, indicate that cvDNA induce a protective siRNA antiviral response against homologous virus infection.

Circular vDNAs Are Chimeras of Viral and LTR-Retrotransposon Sequences

Previous studies indicate that vDNA is largely comprised of truncated genomes and/or chimeric genomes containing LTR-retrotransposon sequences and viral sequences (Goic et al., 2013), and cvDNAs likely comprise a similar heterogeneous population of chimeric, partial, and truncated viral genomes. To characterize this heterogeneous population, we initially cloned and sequenced individual cvDNA molecules. Although both FHV RNA1 and RNA2 produce cvDNA (Figure 1A), our cloning strategy focused on RNA1. Four chimeric cvDNA structures that share common features are shown in Figure 3. Each contains chimeric genotypes formed from discontinuous, subgenomic regions of FHV RNA1 circular DNA and sequences from *Drosophila* retrotransposons. Each of the cvDNAs shared a similar recombination junction around nucleotides 311/957 in FHV RNA1, while two of the four had a second recombination junction around 1,200/2,280 (Figures 3C and 3D). Interestingly, the FHV RNA1 sequences were found in opposite orientation with respect to retrotransposon sequences. This indicates that minus sense viral RNA can also serve as templates for copy-choice recombination during reverse transcription, and rules out a mechanism of vDNA biogenesis whereby viral genomic RNA is co-packaged into retrotransposon VLPs. We tested if our panel of cvDNAs could induce a siRNA response in cells or flies. However, neither FHV-specific transcripts nor siRNAs were detected in naive S2 cells transfected with cvDNA plasmids or in flies inoculated with excised, religated, plasmid-free cvDNAs (data not shown). The lack of response may reflect

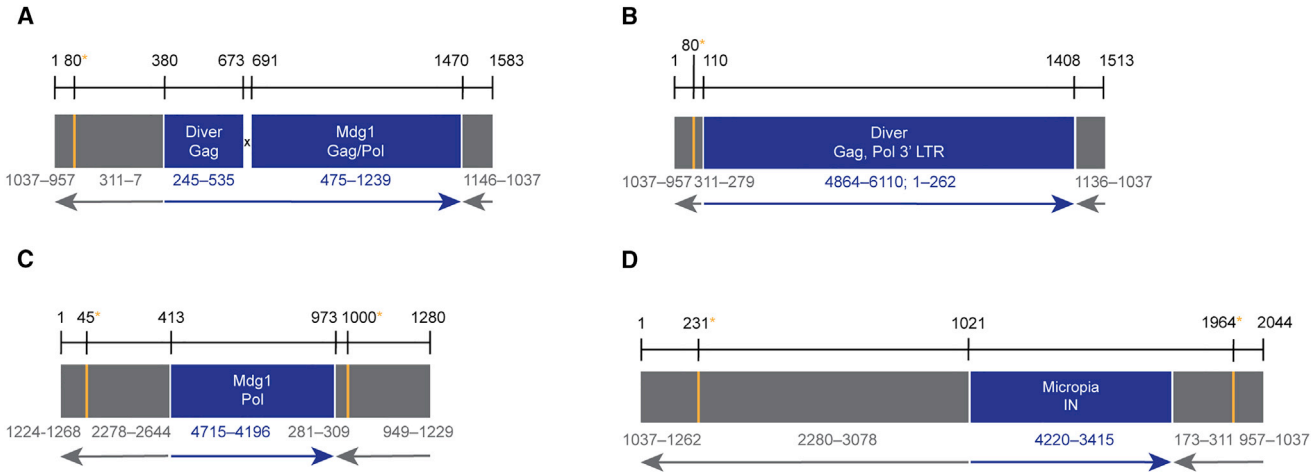

Figure 3. Circular vDNAs Are Chimeras of Viral and LTR-Retrotransposon Sequences

(A–D) Individual cvDNA isolated from FHV-infected S2 cells was cloned and sequenced. Numbers below indicate the nucleotide position in the FHV RNA1 sequence (gray) or in the retrotransposon sequence (blue, with their names). Recombination junctions in FHV are indicated by a vertical orange line. Recombination junctions where at least a 3 nt overlap was present are indicated by asterisks. Arrows indicate the orientation of the sequence with respect to FHV or retrotransposon.

limitations in the quantity, quality, and/or diversity of cvDNA sequences in the transfected cells and inoculated flies.

For more comprehensive genetic characterization of cvDNAs, we undertook an unbiased deep sequencing analysis of circular DNA from FHV-infected and uninfected cells, using a strategy designed to enrich extrachromosomal circular DNA (Lanciano et al., 2017). No reads corresponding to FHV sequences were found in uninfected cells (data not shown). In FHV-infected cells, 8,203 reads had total or partial sequences corresponding to FHV RNA1 and RNA2 (Figure 4A). Of these, 4,023 reads comprised non-continuous FHV sequences, the majority (3,790) containing two non-continuous regions of the FHV genome. The remaining 233 reads were chimeras that matched both FHV and *Drosophila melanogaster* genomes. As *Drosophila* reads in chimeric vDNAs comprise mainly transposon sequences (Goic et al., 2013), we mapped the 233 FHV-*Drosophila* chimeric reads against the transposon database available at Flybase. Fifteen retrotransposons were present in the 133 reads that matched to the transponson database, with *Diver* accounting for 44% of matches (Table S1, related to Figure 4). The chimeric FHV-retrotransposon reads on *Diver* mapped primarily to the LTRs, with some reads mapping to the coding region of the retrotransposon (Figure 4B), suggesting a mechanism for LTR-driven transcription of cvDNA (Beauregard et al., 2008).

The distribution of individual reads along the FHV RNA1 and RNA2 genome was done using both end-to-end and local mapping tools (Figures 4C and 4D). Although reads covered the entirety of RNA1 and RNA2, cvDNA sequences were not uniformly distributed along the FHV genome. This was especially true for RNA1, where there were more reads in the regions between nucleotides 190–300, nucleotides 640–740, and nucleotides 1,060–1,230 (Figure 4C). The skewed distribution was most evident when using the local mapping method, which does not require both ends of the read to match the target genome. This suggests that the non-uniform distribution of FHV sequences in cvDNA is associated with the presence of large quantities of non-continuous viral genomes. To support this, we noted that the regions of RNA1 that were over-represented matched the sequences detected in our four cvDNA clones, where we could identify specific junctions between non-continuous portions of FHV RNA1 (Figure 3). Notably, most of the FHV RNA1 sequences over-represented in cvDNA corresponded to sequences of previously described FHV DVGs (Jaworski and Routh, 2017; Jovel and Schneemann, 2011), raising the possibility that DVGs might be the preferred templates for the cvDNA synthesis.

Defective Genomes Are Templates for vDNA Synthesis and Enhance Antiviral Immunity

To explore the hypothesis that DVGs might be templates for vDNA synthesis, we used Sindbis virus, for which we demonstrated that infected flies produced both vDNA and cvDNA (Figure 1C). In addition, through reverse genetics we are able to extrinsically adjust and intrinsically modify the presence of DVGs (Poirier et al., 2015). Flies were inoculated either with wild-type virus (Sindbis-WT) or with Sindbis-WT supplemented with a previously characterized Sindbis DVG, designated D_G (Poirier et al., 2015). At 7 hr post-infection, total DNA was extracted from individual flies and amplified by PCR using primers specific for Sindbis virus or Sindbis D_G. Sindbis vDNA was amplified from both groups of flies (Figure 5A), while D_G sequences were detected only in flies infected with Sindbis-WT + D_G (Figure 5A, lanes 9 and 12), indicating that DVG is a template for vDNA synthesis. To determine if DVGs are also a template for cvDNA synthesis, DNA from infected flies was treated with DNase-PS and amplified using Sindbis or D_G-specific primers. cvDNA was detected in both groups of flies (Figure 5B): cvDNA corresponding to D_G sequences was detected in Sindbis WT+D_G-infected flies (Figure 5B, lanes 8 and 11), and other cvDNA forms amplified by Sindbis primers were detectable (Figure 5B, lanes 2, 4, 5, 8, and 12). Thus, DVGs can serve as templates for both linear and circular forms of vDNA.

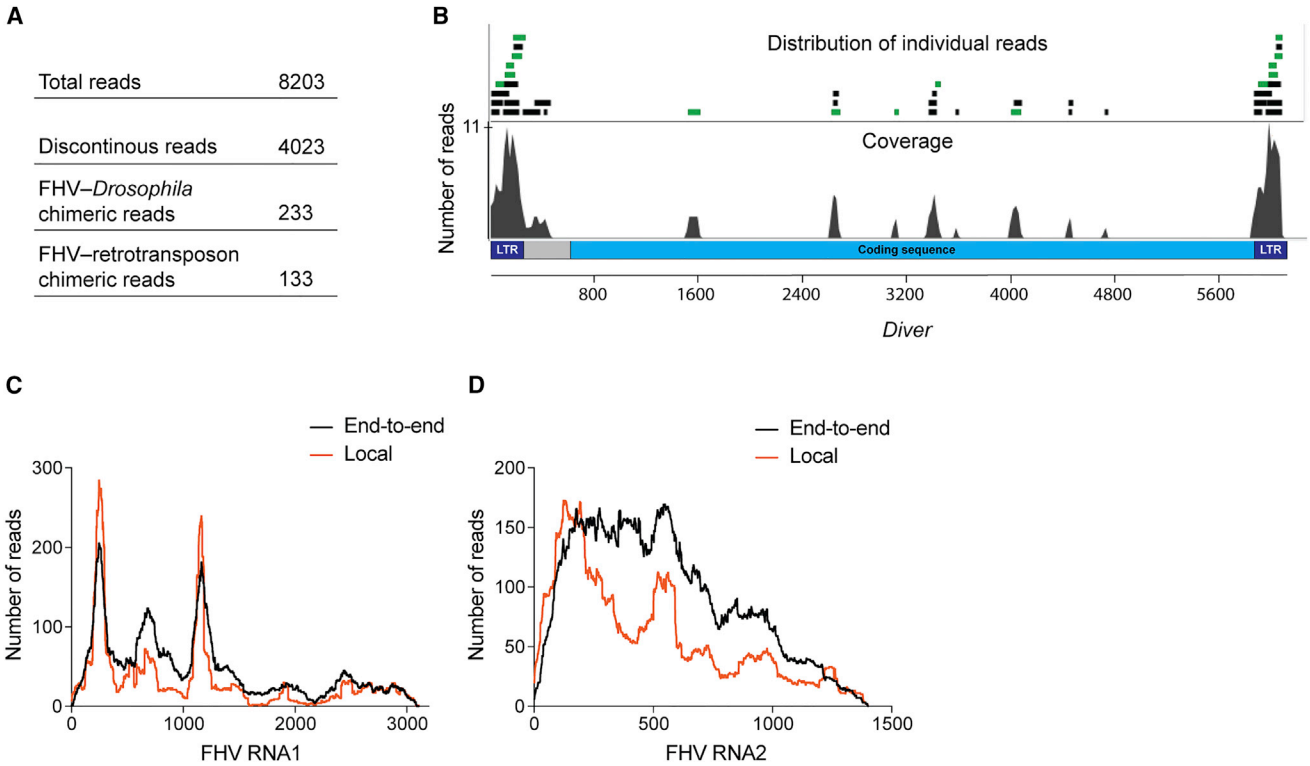

Figure 4. Circular vDNAs Are Chimeras of LTR-Retrotransposons and Viral Sequences Enriched in DVG Sequences

(A) Table presenting the type of reads obtained by deep-sequencing of FHV cvDNAs isolated from infected S2 cells. See also Table S1.

(B) Graph shows distribution of reads and coverage for the LTR and the coding sequence of the retrotransposon *Diver* for the reads "FHV–transposon chimeric read" of (A).

(C and D) Read coverage of cvDNA isolated from FHV-infected S2 cells is represented for FHV RNA1 (C) and RNA2 (D). Reads were mapped with the local (red) or end-to-end method (black).

We next asked whether vDNA synthesized from DVGs can amplify a siRNA-dependent antiviral response *in vivo*, similar to what was observed for vDNA from FHV. Flies were inoculated with Sindbis-WT or with a Sindbis mutant that produces high levels of DVGs (designated Sindbis-highDG). This mutant bears a point mutation in the viral polymerase that leads to higher mutation and recombination rates, and overproduction of DVGs in cell culture (noted as SINV-G in Poirier et al., 2015) and *in vivo* (Figures S2A and S2B, related to Figure 5 and STAR Methods). We infected wild-type and *Ago2*$^{-/-}$ flies with Sindbis-WT or Sindbis-highDG and measured viral titers at sequential times post-infection. In wild-type flies, there was a 4- to 5-fold decrease in virus titer throughout infection with Sindbis-highDG as compared to Sindbis-WT (Figure 5C). However, a similar decrease in virus titer was not observed in *Ago2*$^{-/-}$ flies (Figure 5D), demonstrating that the enhanced antiviral response to Sindbis-highDG was RNAi dependent. As a control, we used a third virus, Sindbis-equalDG, which has the same mutation rate as Sindbis-highDG (Stapleford et al., 2015) but produces DVGs at wild-type levels (Figure S2B, related to Figure 5). Sindbis-equalDG showed similar titers as Sindbis-WT in both wild-type and *Ago2*$^{-/-}$ flies (Figures S2C and S2D, related to Figure 5). This result confirms that overproduction of DVGs triggers the RNAi-dependent decrease in viral load.

Previous studies show that both the Jak-Stat and IMD pathways mediate the Sindbis antiviral response in *Drosophila* (Avadhanula et al., 2009; Dostert et al., 2005). To confirm that the DVG-enhanced antiviral response was specifically RNAi mediated, *hopscotch*$^{-/-}$ and *Rel*$^{-/-}$ mutant flies, which contain mutations in the Jak-stat and Imd pathways, were inoculated with Sindbis-WT or Sindbis-highDG. Similar to wild-type flies, virus titers were reduced in Jak-Stat and IMD mutants infected with Sindbis-highDG as compared to Sindbis-WT infection (Figures S2E and S2F, related to Figure 5). Together with the results in *Ago2*$^{-/-}$ flies (Figure 5D), these data establish that the DVG-enhanced antiviral response depends specifically on an intact RNAi response.

Since DVGs can template for vDNA and cvDNA, and since overproduction of DVGs leads to decreased virus titers in a RNAi-dependent manner, we asked whether DVG-enhanced antiviral response is mediated by vDNA. Flies were fed AZT, a drug that inhibits reverse transcription and synthesis of vDNA (Goic et al., 2013, 2016; Tassetto et al., 2017), and infected with Sindbis-WT or Sindbis-highDG. Treatment of flies with AZT had no effect on virus titers in Sindbis-WT infected flies but largely rescued the drop in titer seen in Sindbis-highDG-infected flies (Figure 5E). This result establishes that the enhanced antiviral response requires production of vDNA and cvDNA from DVGs.

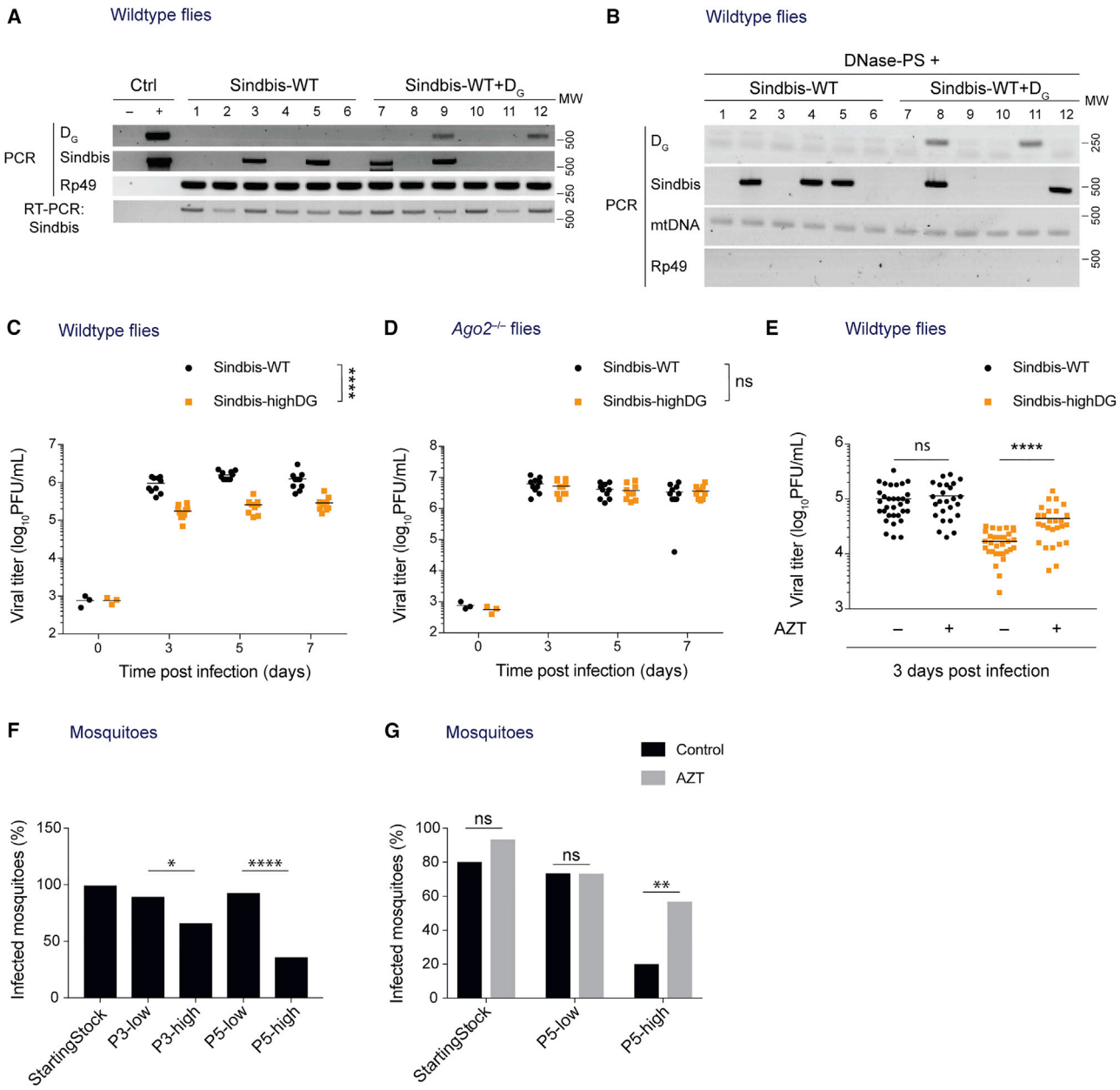

Figure 5. Defective Viral Genomes Are a Preferential Template for Circular vDNA Synthesis and Regulate Viral Load

(A) Wild-type flies were injected with Sindbis-WT or Sindbis-WT+D_G and collected at 7 hr post-infection. Presence of D_G vDNA as well as Sindbis vDNA was assessed in individual flies by PCR. Fly DNA was detected by PCR targeting Rp49, and Sindbis RNA was detected by RT-PCR.

(B) Individual flies were injected with Sindbis-WT or Sindbis-WT+D_G, and DNA was extracted and treated with DNase-PS to isolate circular DNA. cvDNA from Sindbis was amplified in both conditions, while D_G cvDNA was only amplified in Sindbis-WT+D_G-injected flies.

(C) Wild-type flies were injected with Sindbis-WT or Sindbis-highDG and titered individually after infection (0 days post-infection, n = 3 flies) or at 3, 5, and 7 days post-infection (n = 10 flies per condition).

(D) *Ago2*$^{-/-}$ flies were infected as described in (C).

(E) Wild-type flies were fed with AZT or control solution, then infected with Sindbis-WT or Sindbis-highDG and titered 3 days post-infection. Control: Sindbis-WT, n = 32 flies; Sindbis-highDG, n = 31. AZT: Sindbis-WT, n = 25; Sindbis-highDG, n = 27.

(F) *Aedes aegypti* mosquitoes were fed blood meals containing the indicated chikungunya stocks. P3 and P5 indicate number of passages. Low and high indicate passages at low and high MOI, respectively. Mosquitoes (n = 30 per condition) were collected 12 days post-infection, and presence of virus was assessed by plaque assay.

(G) Mosquitoes were fed for a week prior to infection with sucrose supplemented or not with 5 mM AZT, then infected with CHIKV StartingStock, P5-low or P5-high and processed as in (F).

Molecular weights (MW) are indicated. Data are representative of three (A–F) or two (G) independent experiments. Bars show mean. ns, not significant; *$p < 0.05$, **$p < 0.01$, ****$p < 0.0001$ (two-way ANOVA [C and D], Mann-Whitney test [E], or Chi-square test [F and G]). See also Figure S2.

Finally, we tested whether the production of DVGs also modulates the outcome of infection in mosquitoes. Increased proportions of DVGs are produced when RNA virus stocks are passaged at high multiplicity of infection (MOI) (Huang, 1973; Poirier et al., 2015). To generate CHIKV stocks enriched in DVGs, a starting stock was passaged three and five times at low or high MOI to generate stocks with low and high DVG content, respectively. *Aedes aegypti* mosquitoes were then inoculated with these stocks via blood feeding, and the presence of infection was determined in whole mosquitoes after 12 days. The infection rate decreased in mosquitoes fed high MOI/high DVG virus stocks, compared to low MOI/low DVG virus stocks (Figure 5F, P3-high and P5-high compared to P3-low and P5-low). To verify that reduced infectivity was related to vDNA production, mosquitoes were fed AZT a week prior to infection. AZT treatment rescued the decreased infection rate of the P5-high stock (Figure 5G). Together, these experiments demonstrate that high levels of DVGs can enhance antiviral immunity in insects via an RNAi-dependent mechanism that is mediated through vDNA production.

The Helicase Domain of Dcr-2 Regulates the Production of vDNA from Defective Viral Genomes

DVGs are potent stimulators of innate immunity in mammals, acting through RLRs (Sun et al., 2015; Tapia et al., 2013). As the RLRs and Dcr-2 are both members of the DRA family of RNA-dependent ATPases, we hypothesized that the helicase of Dcr-2 in fruit flies may play an important role in the synthesis of vDNA from DVGs, perhaps through RNA binding, sensing, or activation or through recruitment of partner proteins necessary for vDNA biosynthesis. To address this question, we quantified vDNA levels and virus titers in a panel of *Drosophila* Dcr-2 mutants that bear mutations within and outside the helicase domain (Figure 6A) (Lee et al., 2004). We plotted relative vDNA accumulation (measured by qPCR, Figures S3A–S3C, related to Figure 6) versus relative viral loads (measured by plaque assay) for mutant and wild-type flies infected with Sindbis-WT or Sindbis-highDG (Figure 6B and STAR Methods). Certain mutants, such as *Dcr-2*^{G31R}, accumulated more vDNA than wild-type flies, whereas other mutants, such as *Dcr-2*^{A500V}, accumulated 2-fold less vDNA. Across the panel, we found an inverse correlation between levels of vDNA and relative viral load (Figure 6B), indicating that Dcr-2 helicase plays a role in both the synthesis of vDNA from DVGs as well as concomitant reduction in virus load. Since Dcr-2 plays a role in the canonical antiviral siRNA pathway, we determined if the role of Dcr-2 in vDNA synthesis was independent of siRNA production. Indeed, *Dcr-2*^{A500V} and *Dcr-2*^{G31R} flies infected with Sindbis virus produced abundant siRNAs distributed across the virus genome (Figures 6C–6F and S3D–S3G, related to Figure 6). Thus, mutations in Dcr-2 that impact vDNA synthesis have no discernable effect on siRNA production, indicating distinct roles of Dcr-2 in the biosynthesis of vDNA and siRNA production.

The helicase domain of Dcr-2 triggers the antiviral effector Vago independently of antiviral RNAi (Deddouche et al., 2008). Therefore, we tested whether Vago was involved in DVG-mediated decrease of viral titers by infecting *Vago*$^{-/-}$ flies with Sindbis-WT or Sindbis-highDG (Figures S4A and S4B, related to Figure 6). Similar to wild-type flies, *Vago* mutant flies displayed lower viral titers for Sindbis-highDG compared to Sindbis-WT, indicating that Vago was not involved in vDNA biosynthesis.

To see if the Dcr-2 helicase domain interacts with viral RNAs, the helicase domain was cloned in the pAct plasmid and tagged with either FLAG or V5 epitopes. S2 cells were transfected with these constructs and infected with Sindbis-WT or Sindbis-highDG. Cell lysates were immunoprecipitated with anti-FLAG or anti-V5 antibodies, and Sindbis RNA was detected by RT-PCR. Controls included lysates from cells transfected with empty vector or with a vector expressing an unrelated protein (CG4572). We detected amplification products specific for Sindbis virus in the Sindbis-highDG conditions, irrespectively of the tag (Figure 6G), indicating that the helicase domain of Dcr-2 interacts with viral RNA, either through direct binding to viral RNA or via interactions mediated through a partner protein.

The Helicase of Dcr-2 Functions to Modulate vDNA Accumulation and Virus Persistence

The results above reveal that the helicase domain of Dcr-2 is critical for producing vDNA. Furthermore, the outcome of infection would depend on both the level of DVGs in the inoculum and the functional integrity of Dcr-2 in infected flies. To test this, we infected *Dcr-2*^{G31R} and *Dcr-2*^{A500V} flies with Sindbis-WT or with Sindbis-highDG and measured survival. Sindbis-highDG-infected *Dcr-2*^{G31R} flies produced more vDNA and survived longer than Sindbis-WT-infected flies (Figures 7A and 7B). Notably, vDNA accumulation and fly survival were similar between Sindbis-WT and Sindbis-equalDG in *Dcr-2*^{G31R} flies (Figures S5A and S5B, related to Figure 7). In contrast, *Dcr-2*^{A500V} flies, which produce low levels of vDNA, showed no difference in vDNA accumulation (Figure 7C) and died at the same rate with either virus (Figure 7D). Heterozygotes generated from *Dcr-2*^{G31R} and *Dcr-2*^{A500V} crossed with wild-type flies were used to account for variations due to genetic background. Survival of heterozygotes was similar when infected with Sindbis-WT, Sindbis-highDG or Sindbis-equalDG (Figures S5C and S5D, related to Figure 7). The results indicate that viral persistence and fly survival depend on both the Dcr-2-dependent synthesis of vDNA and the quantity of DVGs available to stimulate the vDNA synthesis pathway.

DISCUSSION

In this work, we demonstrate that Dcr-2 plays a critical role mediating two distinct pathways of antiviral immunity in insects: the canonical RNAi pathway and the recently described vDNA amplification pathway. Through its helicase domain, Dcr-2 functions analogous to a PRR to modulate reverse transcription of viral genome products, particularly DVGs, into vDNA. In addition, and through its two RNase III domains, Dcr-2 dices dsRNA to produce siRNAs either from viral origin or from transcripts arising from vDNA transcription. Importantly, we show that modulation of vDNA synthesis by Dcr-2 is independent from the dicing activity: mutants of the helicase domain that alter vDNA production still produce wild-type-like levels of siRNAs. This work provides insights into the mechanism of vDNA biogenesis and establishes strong similarities between insect and mammalian antiviral immunity. In both cases, a RLR helicase domain is required to control viral infection. In insects, Dcr-2 recognition of DVGs activates

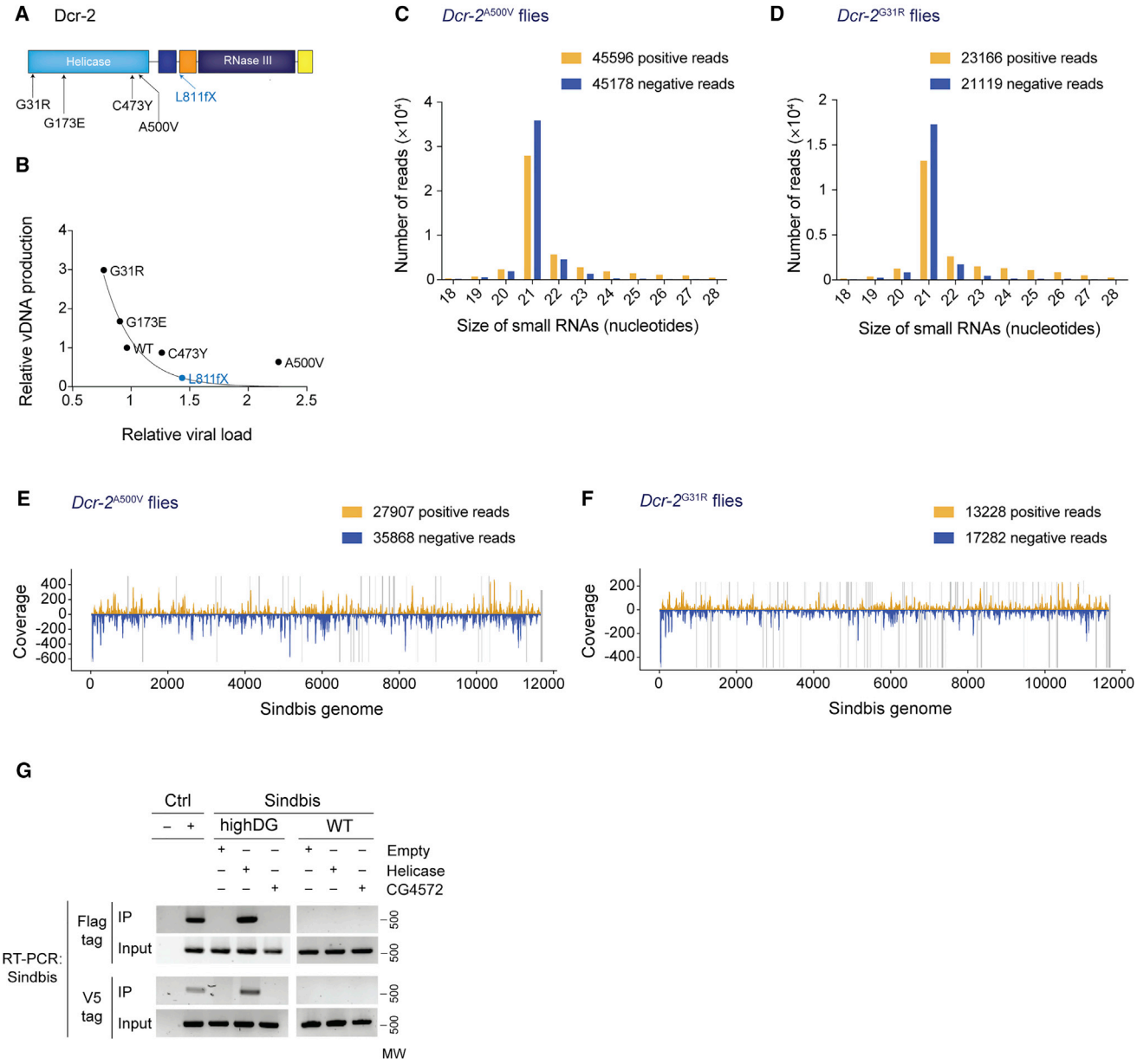

Figure 6. The Helicase Domain of Dicer-2 Regulates the Production of vDNA from Defective Viral Genomes

(A) Schematic of Dcr-2 protein. Point mutations of the helicase domain, as well as the L811fX mutation, which introduces a premature stop codon in the protein, are indicated.

(B) Point mutants of Dcr-2 helicase were injected with Sindbis-WT or Sindbis-highDG and collected 7 hr post-infection. For each virus, vDNA accumulation was measured by qPCR and compared to wild-type flies (n = 8–10 flies, mean of three independent experiments). The y axis of the graph plots the relative ratio mutant/wild-type flies for vDNA accumulation. The same mutants were infected with Sindbis-WT or Sindbis-highDG, and mean titers were measured 3, 5, and 7 days post-infection (n = 10 flies per time point). The relative percentage of Sindbis-highDG titers compared to Sindbis-WT titers as a mutant/wild-type flies ratio is plotted on the x axis (mean of three independent experiments). The relative viral loads quantify the drop in titer of Sindbis-highDG compared to Sindbis-WT in each of the indicated Dcr-2 mutants, presented as a ratio on the value obtained for wild-type flies. Spearman correlation test, $R = -1$, p = 0.016 (*Dcr-2*^{L811fX} mutant, in blue, is not included in the correlation).

(C–F) *Dcr-2*^{A500V} (C and E) or *Dcr-2*^{G31R} (D and F) flies were injected with Sindbis-WT and siRNAs were deep sequenced at 7 days post-infection. Size distribution of reads (C and D) and distribution of 21 nt reads along Sindbis virus genome (E and F) are shown. Uncovered regions are represented as gray lines.

(G) *Drosophila* S2 cells were transfected with a plasmid expressing Dcr-2 helicase tagged with a Flag and V5 tag (helicase), the unrelated protein CG4572 tagged in a similar fashion (CG4572), or the empty plasmid (empty). Cells were then infected with Sindbis-WT or Sindbis-highDG. Before (Input) or after immunoprecipitation with Flag or V5 tag (IP), presence of Sindbis RNA was assessed by RT-PCR. PCR controls (Ctrl) are indicated. Molecular weights (MW) are indicated. Data are representative of two (C–G) independent experiments. See also Figures S3 and S4.

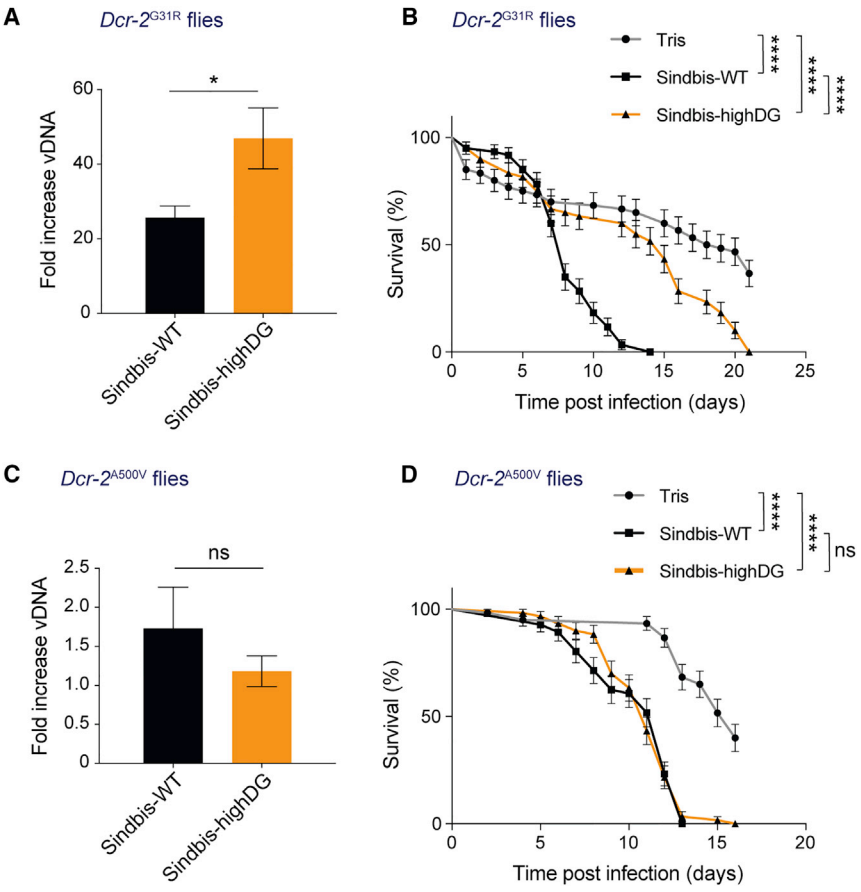

Figure 7. The Helicase Domain of Dcr-2 Modulates vDNA Accumulation and Virus Persistence

(A) *Dcr-2*^{G31R} flies were injected with Sindbis-WT or Sindbis-highDG, and vDNA was measured at 7 hr post-infection by qPCR (n = 20 flies per condition).

(B) *Dcr-2*^{G31R} flies were infected with Sindbis-WT, Sindbis-highDG or mock infected (Tris), and survival was monitored daily (n = 60 flies per condition).

(C) *Dcr-2*^{A500V} flies were processed as in (A).

(D) *Dcr-2*^{A500V} flies were processed as in (B).

(A–D) Bars show mean and SEM, and data are representative of three independent experiments. ns, not significant; *p < 0.05; ****p < 0.0001 (Mann-Whitney test [A and C] or log-rank test [B and D]). See also Figure S5.

both the canonical antiviral RNAi pathway and the vDNA amplification pathway, which leads to persistent viral infection.

The helicase domain of Dcr-2 is phylogenetically close to mammalian RLRs that preferentially bind DVGs during infection, leading to the production of type I interferon (Sun et al., 2015; Tapia et al., 2013). In an analogous manner, our data indicate that the helicase of Dcr-2, together with DVGs, regulates production of vDNA/cvDNA and virus persistence. How Dcr-2 acts to regulate the accumulation of vDNA remains unclear. Based on the related structure of RIG-I (Civril et al., 2011; Colmenares et al., 2007; Luo et al., 2011), all the studied mutations in Dcr-2 are in close proximity to the ATP binding site of the helicase (data not shown). ATP binding by RIG-I results in a conformational change leading to interferon production (Kowalinski et al., 2011). In *Drosophila*, an ATP-dependent conformational change in the helicase domain of Dcr-2 was recently found to play a key role in coordinating the recognition and processive cleavage of blunt-end dsRNA (Sinha et al., 2015, 2017). Thus, recognition and/or cleavage of DVG dsRNA by Dcr-2 helicase might also lead to the activation of vDNA synthesis.

This work further establishes a conserved role of DVGs as PAMPs. The preference of DVGs as PAMPs is likely related to their subcellular localization: full-length viral genomes are better hidden from immune sensors (in membranous invaginations for example), while cytoplasmic DVGs are more available for antiviral sensors and effectors. Indeed, DVGs are preferentially targeted by ADARs during infection in mammals and by RNAi in insects (van den Hoogen et al., 2014; Pfaller et al., 2015; Vodovar et al., 2011; Wu et al., 2010). DVGs of Sendai virus localize diffusely in the cytoplasm of infected cells, while full-length genomes are concentrated in one area (Xu et al., 2017). Because DVGs behave as PAMPs in both insects and mammals, DVGs may be under high selective pressure, which suggests that viruses may have developed specific strategies to regulate their production, as exemplified by the C protein of measles virus or the matrix protein of lymphocytic choriomeningitis virus (Pfaller et al., 2015; Ziegler et al., 2016). A recent publication (Xu et al., 2017) demonstrated that establishment of persistent infection in mammalian cells by paramyxoviruses correlates with high DVG production and activation of interferon through the MAVS signaling platform. More than a byproduct of viral replication, DVGs seem to be a key viral product that can modulate the host immune response and the fate of infection.

While our studies suggest that the helicase domain of Dcr-2 is critical for biosynthesis of vDNA, the molecular events resulting in reverse transcription of DVGs remain elusive. The finding that cvDNA is in opposite orientation with respect to retrotransposon sequences indicates that minus-strand viral RNA can serve as a template for reverse transcription. This, together with evidence that DVGs are the major template for vDNA synthesis, likely rules out reverse transcription of genomic viral RNA in VLPs. Rather, it is more likely that reverse transcription occurs via the translocation of the RT complex to a site enriched in DVGs, such as the RNAi complex. Because Dcr-2 targets both retrotransposon RNA and viral RNA in the cytoplasm, it is tempting to speculate that Dcr-2 acts as a RLR to signal translocation of the RT.

Although we do not fully understand the mechanisms of vDNA biosynthesis, it is clear that both linear and circular vDNA forms are generated during RNA virus infection. The cvDNA forms were stable and persisted at least 2 weeks after infection, suggesting their importance in vDNA immune response pathway. Inoculation of flies with cvDNA resulted in increased survival, but not a

concomitant decrease in virus titer. Virus titers or RNA copies do not always reflect on the fitness cost of virus infection in insects, which are commonly measured by survival, fecundity, fertility, and other more qualitative phenotypic observations. This is especially so in lab colonies, which live under ideal environmental conditions (Maciel-de-Freitas et al., 2011). Greater insight into mechanisms of viral pathogenesis during persistent infections is needed to understand the relationship between virus titer and persistence and/or healthy carrier versus non-healthy carrier phenotype.

This cvDNA may be the precursor of integration of viral sequences into host genomes. These integrations, referred to as endogenous viral elements, were recently associated with retrotransposons in the mosquito genome (Crochu et al., 2004; Palatini et al., 2017; Suzuki et al., 2017). In addition to their role in antiviral immunity shown here, circular DNA is commonly found in a number of species, including *C. elegans* and *Mus musculus*, and in human cell lines (Cohen et al., 2003; Shoura et al., 2017). Circular DNA has recently garnered growing attention as a key molecule in health and disease and in regulation of cell communication and cell function (Pennisi, 2017).

Finally, our work demonstrates that virus persistence in insects is dependent on the levels of vDNA produced, which can be modulated either through AZT treatment, through increased levels of DVGs, and/or by mutation of Dcr-2 helicase domain. As such, our work opens the possibility that strategies to modulate levels of vDNA may help control arboviral infection in the insect host. Toward that end, additional studies to optimize and more fully examine the mechanism of cvDNA-mediated control of RNA virus infection are ongoing.

STAR★METHODS

Detailed methods are provided in the online version of this paper and include the following:

SUPPLEMENTAL INFORMATION

Supplemental Information includes five figures and three tables and can be found with this article at https://doi.org/10.1016/j.chom.2018.02.001.

ACKNOWLEDGMENTS

We thank the Saleh and Vignuzzi labs, especially V. Mongelli, L. Carrau, and G. Moratorio for scientific advice, and B. tenOever for discussions. We thank Jean-Luc Imler for the various fly strains. We thank Catherine Lallemand for mosquito rearing and Alongkot Ponlawat for field collection of mosquitoes. Work was supported by the French Government's Investissement d'Avenir program, Laboratoire d'Excellence Integrative Biology of Emerging Infectious Diseases (grant ANR-10-LABX-62-IBEID to L.L., M.V., and M.-C.S.), the European Research Council (FP7/2013-2019 ERC CoG 615220 to M.-C.S.), and the DARPA INTERCEPT program managed by Dr. Jim Gimlett and administered though DARPA Cooperative Agreement #HR0011-17-2-0023 to M.V. and M.-C.S. (the content of the information does not necessarily reflect the position or the policy of the U.S. government, and no official endorsement should be inferred). L.L. was supported by the City of Paris Emergence(s) program in Biomedical Research (grant DASES 2013-33) and by the European Union's Horizon 2020 research and innovation program under ZikaPLAN grant agreement No. 734584. L.T.-P. is a Marie Skłodowska-Curie actions fellow (H2020 MSCA-IF 656398-DDRR).

AUTHOR CONTRIBUTIONS

Conceptualization: E.Z.P., B.G., L.T.-P., L.F., S.C., M.V., and M.-C.S.; Investigation: E.Z.P., B.G., L.T.-P, L.I.L., T.V., H.L., V.G., S.L., C.B., S.M., H.B., M.M., S.C., and M.-C.S.; Software: J.B. and L.F.; Formal analysis: E.Z.P., J.B., and L.F.; Writing: E.Z.P., S.C., M.V., and M.-C.S.; Resources: L.L.; Funding acquisition: L.L., M.V., and M.-C.S.

DECLARATION OF INTERESTS

The authors declare no competing interests.

Received: May 17, 2017
Revised: November 8, 2017
Accepted: February 7, 2018
Published: March 1, 2018

REFERENCES

Aaskov, J., Buzacott, K., Thu, H.M., Lowry, K., and Holmes, E.C. (2006). Long-term transmission of defective RNA viruses in humans and Aedes mosquitoes. Science *311*, 236–238.

Avadhanula, V., Weasner, B.P., Hardy, G.G., Kumar, J.P., and Hardy, R.W. (2009). A novel system for the launch of alphavirus RNA synthesis reveals a role for the Imd pathway in arthropod antiviral response. PLoS Pathog. *5*, e1000582.

Baum, A., Sachidanandam, R., and García-Sastre, A. (2010). Preference of RIG-I for short viral RNA molecules in infected cells revealed by next-generation sequencing. Proc. Natl. Acad. Sci. USA *107*, 16303–16308.

Beauregard, A., Curcio, M.J., and Belfort, M. (2008). The take and give between retrotransposable elements and their hosts. Annu. Rev. Genet. *42*, 587–617.

Bredenbeek, P.J., Frolov, I., Rice, C.M., and Schlesinger, S. (1993). Sindbis virus expression vectors: packaging of RNA replicons by using defective helper RNAs. J. Virol. *67*, 6439–6446.

Civril, F., Bennett, M., Moldt, M., Deimling, T., Witte, G., Schiesser, S., Carell, T., and Hopfner, K.-P. (2011). The RIG-I ATPase domain structure reveals insights into ATP-dependent antiviral signalling. EMBO Rep. *12*, 1127–1134.

Coffey, L.L., and Vignuzzi, M. (2011). Host alternation of chikungunya virus increases fitness while restricting population diversity and adaptability to novel selective pressures. J. Virol. *85*, 1025–1035.

Cohen, S., Yacobi, K., and Segal, D. (2003). Extrachromosomal circular DNA of tandemly repeated genomic sequences in Drosophila. Genome Res. *13* (6A), 1133–1145.

Colmenares, S.U., Buker, S.M., Buhler, M., Dlakić, M., and Moazed, D. (2007). Coupling of double-stranded RNA synthesis and siRNA generation in fission yeast RNAi. Mol. Cell *27*, 449–461.

Crochu, S., Cook, S., Attoui, H., Charrel, R.N., De Chesse, R., Belhouchet, M., Lemasson, J.J., de Micco, P., and de Lamballerie, X. (2004). Sequences of flavivirus-related RNA viruses persist in DNA form integrated in the genome of Aedes spp. mosquitoes. J. Gen. Virol. *85*, 1971–1980.

Cunningham, T.P., Montelaro, R.C., and Rushlow, K.E. (1993). Lentivirus envelope sequences and proviral genomes are stabilized in Escherichia coli when cloned in low-copy-number plasmid vectors. Gene *124*, 93–98.

Deddouche, S., Matt, N., Budd, A., Mueller, S., Kemp, C., Galiana-Arnoux, D., Dostert, C., Antoniewski, C., Hoffmann, J.A., and Imler, J.-L. (2008). The DExD/H-box helicase Dicer-2 mediates the induction of antiviral activity in drosophila. Nat. Immunol. *9*, 1425–1432.

Dostert, C., Jouanguy, E., Irving, P., Troxler, L., Galiana-Arnoux, D., Hetru, C., Hoffmann, J.A., and Imler, J.-L. (2005). The Jak-STAT signaling pathway is required but not sufficient for the antiviral response of drosophila. Nat. Immunol. *6*, 946–953.

Frolova, E.I., Gorchakov, R., Pereboeva, L., Atasheva, S., and Frolov, I. (2010). Functional Sindbis virus replicative complexes are formed at the plasma membrane. J. Virol. *84*, 11679–11695.

Galiana-Arnoux, D., Dostert, C., Schneemann, A., Hoffmann, J.A., and Imler, J.-L. (2006). Essential function in vivo for Dicer-2 in host defense against RNA viruses in drosophila. Nat. Immunol. *7*, 590–597.

Goic, B., Vodovar, N., Mondotte, J.A., Monot, C., Frangeul, L., Blanc, H., Gausson, V., Vera-Otarola, J., Cristofari, G., and Saleh, M.-C. (2013). RNA-mediated interference and reverse transcription control the persistence of RNA viruses in the insect model Drosophila. Nat. Immunol. *14*, 396–403.

Goic, B., Stapleford, K.A., Frangeul, L., Doucet, A.J., Gausson, V., Blanc, H., Schemmel-Jofre, N., Cristofari, G., Lambrechts, L., Vignuzzi, M., and Saleh, M.C. (2016). Virus-derived DNA drives mosquito vector tolerance to arboviral infection. Nat. Commun. *7*, 12410.

Grimley, P.M., Levin, J.G., Berezesky, I.K., and Friedman, R.M. (1972). Specific membranous structures associated with the replication of group A arboviruses. J. Virol. *10*, 492–503.

Huang, A.S. (1973). Defective interfering viruses. Annu. Rev. Microbiol. *27*, 101–117.

Hughes, S.H. (2015). Reverse transcription of retroviruses and LTR retrotransposons. Microbiol. Spectr. *3*, MDNA3-0027-2014.

Jaworski, E., and Routh, A. (2017). Parallel ClickSeq and Nanopore sequencing elucidates the rapid evolution of defective-interfering RNAs in Flock House virus. PLoS Pathog. *13*, e1006365.

Jovel, J., and Schneemann, A. (2011). Molecular characterization of Drosophila cells persistently infected with Flock House virus. Virology *419*, 43–53.

Kowalinski, E., Lunardi, T., McCarthy, A.A., Louber, J., Brunel, J., Grigorov, B., Gerlier, D., and Cusack, S. (2011). Structural basis for the activation of innate immune pattern-recognition receptor RIG-I by viral RNA. Cell *147*, 423–435.

Lanciano, S., Carpentier, M.-C., Llauro, C., Jobet, E., Robakowska-Hyzorek, D., Lasserre, E., Ghesquière, A., Panaud, O., and Mirouze, M. (2017). Sequencing the extrachromosomal circular mobilome reveals retrotransposon activity in plants. PLoS Genet. *13*, e1006630.

Langmead, B., Trapnell, C., Pop, M., and Salzberg, S.L. (2009). Ultrafast and memory-efficient alignment of short DNA sequences to the human genome. Genome Biol. *10*, R25.

Lazzarini, R.A., Keene, J.D., and Schubert, M. (1981). The origins of defective interfering particles of the negative-strand RNA viruses. Cell *26*, 145–154.

Lee, Y.S., Nakahara, K., Pham, J.W., Kim, K., He, Z., Sontheimer, E.J., and Carthew, R.W. (2004). Distinct roles for Drosophila Dicer-1 and Dicer-2 in the siRNA/miRNA silencing pathways. Cell *117*, 69–81.

Lequime, S., Fontaine, A., Ar Gouilh, M., Moltini-Conclois, I., and Lambrechts, L. (2016). Genetic drift, purifying selection and vector genotype shape dengue virus intra-host genetic diversity in mosquitoes. PLoS Genet. *12*, e1006111.

Li, H., Li, W.X., and Ding, S.W. (2002). Induction and suppression of RNA silencing by an animal virus. Science *296*, 1319–1321.

Li, C., Vagin, V.V., Lee, S., Xu, J., Ma, S., Xi, H., Seitz, H., Horwich, M.D., Syrzycka, M., Honda, B.M., et al. (2009). Collapse of germline piRNAs in the absence of Argonaute3 reveals somatic piRNAs in flies. Cell *137*, 509–521.

Liu, J., Carmell, M.A., Rivas, F.V., Marsden, C.G., Thomson, J.M., Song, J.J., Hammond, S.M., Joshua-Tor, L., and Hannon, G.J. (2004). Argonaute2 is the catalytic engine of mammalian RNAi. Science *305*, 1437–1441.

Luo, D., Ding, S.C., Vela, A., Kohlway, A., Lindenbach, B.D., and Pyle, A.M. (2011). Structural insights into RNA recognition by RIG-I. Cell *147*, 409–422.

Luo, D., Kohlway, A., and Pyle, A.M. (2013). Duplex RNA activated ATPases (DRAs): platforms for RNA sensing, signaling and processing. RNA Biol. *10*, 111–120.

Maciel-de-Freitas, R., Koella, J.C., and Lourenço-de-Oliveira, R. (2011). Lower survival rate, longevity and fecundity of Aedes aegypti (Diptera: Culicidae) females orally challenged with dengue virus serotype 2. Trans. R. Soc. Trop. Med. Hyg. *105*, 452–458.

Marriott, A.C., and Dimmock, N.J. (2010). Defective interfering viruses and their potential as antiviral agents. Rev. Med. Virol. *20*, 51–62.

McKnight, K.L., Simpson, D.A., Lin, S.-C., Knott, T.A., Polo, J.M., Pence, D.F., Johannsen, D.B., Heidner, H.W., Davis, N.L., and Johnston, R.E. (1996). Deduced consensus sequence of Sindbis virus strain AR339: mutations contained in laboratory strains which affect cell culture and in vivo phenotypes. J. Virol. *70*, 1981–1989.

Miller, D.J., Schwartz, M.D., and Ahlquist, P. (2001). Flock house virus RNA replicates on outer mitochondrial membranes in Drosophila cells. J. Virol. *75*, 11664–11676.

Morgan, M., and Grimshaw, A. (2009). High-throughput computing in the sciences. Methods Enzymol. *467*, 197–227.

Nan, Y., Nan, G., and Zhang, Y.-J. (2014). Interferon induction by RNA viruses and antagonism by viral pathogens. Viruses *6*, 4999–5027.

Okamura, K., Ishizuka, A., Siomi, H., and Siomi, M.C. (2004). Distinct roles for Argonaute proteins in small RNA-directed RNA cleavage pathways. Genes Dev. *18*, 1655–1666.

Palatini, U., Miesen, P., Carballar-Lejarazu, R., Ometto, L., Rizzo, E., Tu, Z., van Rij, R.P., and Bonizzoni, M. (2017). Comparative genomics shows that viral integrations are abundant and express piRNAs in the arboviral vectors Aedes aegypti and Aedes albopictus. BMC Genomics *18*, 512.

Paro, S., Imler, J.-L., and Meignin, C. (2015). Sensing viral RNAs by Dicer/RIG-I like ATPases across species. Curr. Opin. Immunol. *32*, 106–113.

Pennisi, E. (2017). Circular DNA throws biologists for a loop. Science *356*, 996.

Pfaller, C.K., Mastorakos, G.M., Matchett, W.E., Ma, X., Samuel, C.E., and Cattaneo, R. (2015). Measles virus defective interfering RNAs are generated frequently and early in the absence of C protein and can be destabilized by adenosine deaminase acting on RNA-1-like hypermutations. J. Virol. *89*, 7735–7747.

Poirier, E.Z., Mounce, B.C., Rozen-Gagnon, K., Hooikaas, P.J., Stapleford, K.A., Moratorio, G., and Vignuzzi, M. (2015). Low-fidelity polymerases of alphaviruses recombine at higher rates to overproduce defective interfering particles. J. Virol. *90*, 2446–2454.

Reed, L.J., and Muench, H. (1938). A simple method of estimating fifty per cent endpoints. Am. J. Hyg. *27*, 493–497.

Rozen-Gagnon, K., Stapleford, K.A., Mongelli, V., Blanc, H., Failloux, A.-B., Saleh, M.-C., and Vignuzzi, M. (2014). Alphavirus mutator variants present

host-specific defects and attenuation in mammalian and insect models. PLoS Pathog. *10*, e1003877.

Saleh, M.-C., Tassetto, M., van Rij, R.P., Goic, B., Gausson, V., Berry, B., Jacquier, C., Antoniewski, C., and Andino, R. (2009). Antiviral immunity in Drosophila requires systemic RNA interference spread. Nature *458*, 346–350.

Sanchez David, R.Y., Combredet, C., Sismeiro, O., Dillies, M.-A., Jagla, B., Coppée, J.-Y., Mura, M., Guerbois Galla, M., Despres, P., Tangy, F., and Komarova, A.V. (2016). Comparative analysis of viral RNA signatures on different RIG-I-like receptors. Elife *5*, e11275.

Shoura, M., Gabdank, I., Hansen, L., Merker, J., Gotlib, J., Levene, S., and Fire, A. (2017). Beyond the linear genome: comprehensive determination of the endogenous circular elements in C. elegans and human genomes via an unbiased genomic-biophysical method. bioRxiv. Published online April 19, 2017. https://doi.org/10.1101/128686.

Simon-Loriere, E., and Holmes, E.C. (2011). Why do RNA viruses recombine? Nat. Rev. Microbiol. *9*, 617–626.

Sinha, N.K., Trettin, K.D., Aruscavage, P.J., and Bass, B.L. (2015). Drosophila dicer-2 cleavage is mediated by helicase- and dsRNA termini-dependent states that are modulated by Loquacious-PD. Mol. Cell *58*, 406–417.

Sinha, N.K., Iwasa, J., Shen, P.S., and Bass, B.L. (2017). Dicer uses distinct modules for recognizing dsRNA termini. Science *359*, 329–334.

Stapleford, K.A., Rozen-Gagnon, K., Das, P.K., Saul, S., Poirier, E.Z., Blanc, H., Vidalain, P.-O., Merits, A., and Vignuzzi, M. (2015). Viral polymerase-helicase complexes regulate replication fidelity to overcome intracellular nucleotide depletion. J. Virol. *89*, 11233–11244.

Sun, Y., Jain, D., Koziol-White, C.J., Genoyer, E., Gilbert, M., Tapia, K., Panettieri, R.A., Jr., Hodinka, R.L., and López, C.B. (2015). Immunostimulatory defective viral genomes from respiratory syncytial virus promote a strong innate antiviral response during infection in mice and humans. PLoS Pathog. *11*, e1005122.

Suzuki, Y., Frangeul, L., Dickson, L.B., Blanc, H., Verdier, Y., Vinh, J., Lambrechts, L., and Saleh, M.-C. (2017). Uncovering the Repertoire of endogenous flaviviral elements in aedes mosquito genomes. J. Virol. *91*, e00571-17.

Tapia, K., Kim, W.K., Sun, Y., Mercado-López, X., Dunay, E., Wise, M., Adu, M., and López, C.B. (2013). Defective viral genomes arising in vivo provide critical danger signals for the triggering of lung antiviral immunity. PLoS Pathog. *9*, e1003703.

Tassetto, M., Kunitomi, M., and Andino, R. (2017). Circulating immune cells mediate a systemic RNAi-based adaptive antiviral response in *Drosophila*. Cell *169*, 314–325.

Tomari, Y., Du, T., and Zamore, P.D. (2007). Sorting of *Drosophila* small silencing RNAs. Cell *130*, 299–308.

van den Hoogen, B.G., van Boheemen, S., de Rijck, J., van Nieuwkoop, S., Smith, D.J., Laksono, B., Gultyaev, A., Osterhaus, A.D.M.E., and Fouchier, R.A.M. (2014). Excessive production and extreme editing of human metapneumovirus defective interfering RNA is associated with type I interferon induction. J. Gen. Virol. *95*, 1625–1633.

van Rij, R.P., Saleh, M.-C., Berry, B., Foo, C., Houk, A., Antoniewski, C., and Andino, R. (2006). The RNA silencing endonuclease Argonaute 2 mediates specific antiviral immunity in Drosophila melanogaster. Genes Dev. *20*, 2985–2995.

Vodovar, N., Goic, B., Blanc, H., and Saleh, M.-C. (2011). In silico reconstruction of viral genomes from small RNAs improves virus-derived small interfering RNA profiling. J. Virol. *85*, 11016–11021.

Wu, Q., Luo, Y., Lu, R., Lau, N., Lai, E.C., Li, W.-X., and Ding, S.-W. (2010). Virus discovery by deep sequencing and assembly of virus-derived small silencing RNAs. Proc. Natl. Acad. Sci. USA *107*, 1606–1611.

Xu, J., Sun, Y., Li, Y., Ruthel, G., Weiss, S.R., Raj, A., Beiting, D., and López, C.B. (2017). Replication defective viral genomes exploit a cellular pro-survival mechanism to establish paramyxovirus persistence. Nat. Commun. *8*, 799.

Yount, J.S., Kraus, T.A., Horvath, C.M., Moran, T.M., and López, C.B. (2006). A novel role for viral-defective interfering particles in enhancing dendritic cell maturation. J. Immunol. *177*, 4503–4513.

Yount, J.S., Gitlin, L., Moran, T.M., and López, C.B. (2008). MDA5 participates in the detection of paramyxovirus infection and is essential for the early activation of dendritic cells in response to Sendai Virus defective interfering particles. J. Immunol. *180*, 4910–4918.

Ziegler, C.M., Eisenhauer, P., Bruce, E.A., Weir, M.E., King, B.R., Klaus, J.P., Krementsov, D.N., Shirley, D.J., Ballif, B.A., and Botten, J. (2016). The lymphocytic choriomeningitis virus matrix protein PPXY late domain drives the production of defective interfering particles. PLoS Pathog. *12*, e1005501.

STAR★METHODS

KEY RESOURCES TABLE

REAGENT or RESOURCE	SOURCE	IDENTIFIER
Antibodies		
Anti-V5	Invitrogen	R96025
Anti-Flag M2 Magnetic Beads	Sigma Aldrich	M8823
Bacterial and Virus Strains		
Flock House virus	Obtained from Annette Schneemann (The Scripps Research Institute)	N/A
Drosophila C virus	Obtained from Jean-Luc Imler (University of Strasbourg)	
Sindbs virus (strain AR339)	(McKnight et al., 1996)	N/A
Sindbis-highDG	(Rozen-Gagnon et al., 2014)	N/A
Sindbis-equalDG	(Stapleford et al., 2015)	N/A
chikungunya virus (06-049)	(Coffey and Vignuzzi, 2011)	N/A
Chemicals, Peptides, and Recombinant Proteins		
Azidothymidine (AZT)	Sigma Aldrich	A2169
Critical Commercial Assays		
mMachine mMessage Transcription Kit	Thermo Fisher Scientific	AM1340
Phusion High FIdelity DNA polymerase	NEB	M0530S
Plasmid-Safe ATP-dependent DNase	Epicenter	E3101K
Power SYBR Green Master Mix	Thermo Fisher Scientific	4368577
Trizol	Thermo Fisher Scientific	15596018
Maxima H Minus First Strand cDNA synthesis kit	Thermo Fisher Scientific	K1681
Illustra TempliPhi kit	GE Healthcare	25640010
PicoGreen	Invitrogen	P7589
Nextera XT library kit	Illumina	FC-131-1024
DNA Bioanalyzer chip	Agilent Technologies	5067-1505
Turbo DNA-free kit	Life technologie	AM1907
NEBNext Multiplex Small RNA Library Prep	Illumina	E7300S
Deposited Data		
SRA	PRJNA387403	DNA seq of circular DNA from Drosophila S2 cells infected or not with FHV
	PRJNA387406	Small RNAs of Drosophila w^{1118} flies inoculated or not with FHV or circular-viral-DNA of FHV
	PRJNA416764	RNA seq of Drosophila *Dicer-2*^{L811fX} flies infected with Sindbis-WT, Sindbis-highDG or Sindbis-equalDG viruses
	PRJNA416718	Small RNAs of *Drosophila melanogaster* Dicer-2 mutant flies infected with Sindbis-WT virus
Experimental Models: Cell Lines		
Drosophila S2 cells	Invitrogen	R69007
BHK-21 cells [C13]	Sigma-Aldrich	85011433-1VL
Vero cells	Sigma-Aldrich	84113001-1VL
Experimental Models: Organisms/Strains		
D. melanogaster. Wildtype: *w[1118]*	Bloomington Drosophila Stock Center	BDSC: 3605
D. melanogaster. Ago-2 mutant: *w* ; Ago-2[414]*	Okamura et al., 2004	Kyoto: 109027

(*Continued on next page*)

Continued

REAGENT or RESOURCE	SOURCE	IDENTIFIER
D. melanogaster. Hopscotch mutant: *y[1] hop[m38]/FM7c*	Gift from JL Imler	N/A
D. melanogaster. Hopscotch mutant: *hop[mv1]/x^x v+ yy+*	Gift from JL Imler	N/A
D. melanogaster. Relish mutant: *w[1118] ;; Df(3) E[20i] rel*	Gift from JL Imler	N/A
D. melanogaster. Dicer-2 mutant: *y[d2] w[1118], P{ry$^{+t7.2}$ = ey–FLP.N}2 ; Dcr-2[L811fX]*	(Tomari et al., 2007)	N/A
D. melanogaster. Dicer-2 helicase mutant: *yw ; Dcr-2[G31R]*	(Lee et al., 2004) Gift from JL Imler	N/A
D. melanogaster. Dicer-2 helicase mutant: *yw ; Dcr-2[G173E]*	(Lee et al., 2004) Gift from JL Imler	N/A
D. melanogaster. Dicer-2 helicase mutant: *yw ; Dcr-2[C473Y]*	(Lee et al., 2004) Gift from JL Imler	N/A
D. melanogaster. Dicer-2 helicase mutant: *yw ; Dcr-2[A500V]*	(Lee et al., 2004) Gift from JL Imler	N/A
D. melanogaster. *Vago[ΔM10]*:	(Deddouche et al., 2008) Gift from JL Imler	N/A
D. melanogaster. Vago control strain	(Deddouche et al., 2008) Gift from JL Imler	N/A
Aedes aegypti. Wildtype collected in Thailand	(Lequime et al., 2016)	N/A
Oligonucleotides		
Sindbis virus 414F	Eurogentec	AAGGATCTCCGGACCGTACT
Sindbis virus 913R	Eurogentec	CCTTCGCAACTCACCACTGT
FHV RNA1 69F	Eurogentec	CCAGATCACCCGAACTGAAT
FHV RNA1 1002R	Eurogentec	CGACCGATGGAAACCAGCAGTTC
FHV RNA2 70F	Eurogentec	CGTCACAACAACCCAAACAG
FHV RNA2 701R	Eurogentec	CCACCGCTAGAACACCATCT
DCV 3133F	Eurogentec	GTTGCCTTATCTGCTCTG
DCV 4328R	Eurogentec	CGCATAACCATGCTCTTCTG
DCV 4235F	Eurogentec	CGACTCGTACTGGGGATTGT
DCV 4863R	Eurogentec	AGGAAATCCTGGTGACGTTG
Software and Algorithms		
R	R Core Team	http://www.R-project.org/
Graphpad Prism	Graphpad	https://www.graphpad.com/
FastQC	FastQC	http://www.bioinformatics.babraham.ac.uk/projects/fastqc/
Cutadapt	Cutadapt	https://cutadapt.readthedocs.io/en/stable/
Other		
Nanoject II injector	Drummond Scientific	3-000-204

CONTACT FOR REAGENT AND RESOURCE SHARING

Further information and requests for resources and reagents should be directed to Maria-Carla Saleh (carla.saleh@pasteur.fr).

EXPERIMENTAL MODEL AND SUBJECT DETAILS

Fly and mosquito stocks

The following fly stocks were used: *w^{1118}* (Bloomington), *Ago-2^{414}* (Okamura et al., 2004), *y^{1} hop^{m38}/FM7c* (J.-L. Imler), *hop^{mv1}/x^x v^{+} yy^{+}* (J.-L. Imler), *w^{1118} ; ; Df(3) E^{20i} rel* (J.-L. Imler), *y^{d2} w^{1118}; P{ry$^{+t7.2}$ = ey–FLP.N}2 ; Dcr-2^{L811fX}* (obtained from P. Zamore, (Tomari et al., 2007)), *yw ; Dcr-2^{G31R}*, *yw ; Dcr-2^{G173E}*, *yw ; Dcr-2^{C473Y}*, *yw ; Dcr-2^{A500V}* (4 strains obtained from J-L. Imler, described in Lee et al., 2004), Vago control and *Vago^{ΔM10}* from J.-L. Imler (Deddouche et al., 2008). Hopscotch homozygotes knock-out flies were

obtained by crossing y^1 hop^{m38}/FM7c virgins and hop^{mv1}/x^x v^+ yy^+ males. All lines were tested for the presence of *Wolbachia*, and treated with 0.05 mg/ml tetracycline if necessary. All flies were regularly tested by RT-PCR for NoV, CrPV, DAV, DXV, DCV and FHV. Flies were reared on standard medium at 25°C, in tubes containing around 50 flies. All experiments were performed with 4-6-day-old female flies, to be consistent with other studies (Goic et al., 2013; Saleh et al., 2009). Experiments were performed 3 independent times. Flies or mosquitoes were always analyzed individually except for small RNAs deep-sequencing. Titration experiments featured 10 individual flies - each plotted by a single dot - per time point (except at t = 0 hr post-infection, n = 3 flies) and were analyzed with ANOVA (excluding t = 0 time point, $\alpha = 0.05$). Survival experiments were done with 3 replicates in individual tubes, each tube containing 25 flies (75 flies total, Figure 1) or 20 flies (60 flies total, Figures 7 and S5). Log-rank (Mantel-Cox) test was performed. Other experiments were tested using two-tailed Mann-Withney test, a non-parametric test, with a threshold at 0.05. Mean and standard error from the mean (SEM) are indicated in the graphs.

Aedes aegypti female mosquitoes belonged to the 7th generation of a colony derived from wild *Aedes aegypti* collected in Kamphaeng Phet Province, Thailand. Mosquitoes were grown at 28°C and fed with 10% sucrose. A day prior blood feeding, females were selected and starved for a day. For each experiment, 30 individual mosquitoes were titrated per condition. Initial experiment (Figure 5F) was repeated 3 independent times and AZT rescue experiment was repeated two independent times (Figure 5G). Results were analyzed using a Fisher's exact test, with $\alpha = 0.05$.

Viruses and Cells

Drosophila S2 cells (Invitrogen) were cultured in Schneider's *Drosophila* medium supplemented with 1% Penicillin-Streptomycin (P-S, Sigma) and 10% fetal calf serum, at 25°C. BHK-21 cells and Vero cells were maintained in Dulbelcco's modified Eagle's medium (DMEM, GIBCO) supplemented with 10% newborn calf serum (NCS, GIBCO) and 1% P-S at 37°C with 5% CO_2.

Sindbis was produced from the pTR339 infectious clone and CHIKV from the 06-049 infectious clone. Sindbis replicon was produced from the pSINrep5 clone (Bredenbeek et al., 1993). Viral RNA was *in vitro* transcribed using the mMessage mMachine SP6 kit (Thermo Fisher Scientific) and 10 μg RNA was electroporated in BHK-21 cells in an XCell Gene Pulser Biorad. These electroporations were used to infect BHK-21 cells to give a stock of virus that was titered by plaque assay on Vero cells. Briefly, 24-well plates were seeded with 2×10^5 Vero cells and infected with 10-fold dilutions of each sample, before being overlaid with DMEM containing 2% NCS and 0.8% agarose. Cells were fixed with formaline at 48 hr post-infection for Sindbis and 72 hr for CHIKV and stained with crystal violet. Stock viruses were passaged at MOI 1 (low MOI) or at MOI 25 (high MOI) in BHK-21 cells, and titered by plaque assay. Stocks of Sindbis-WT, Sindbis-highDG and Sindbis-equalDG were concentrated by ultracentrifugation on 20% sucrose cushion, 2 hr at 107,000 × *g* using a SW41 Ti rotor in an Optima XPN-100 centrifuge (Beckman Coulter). Point mutations of low fidelity variants were resequenced in stocks and in flies 7 days post-infection.

Sindbis replicon was produced by electroporating 5 μg of replicon RNA and 5 μg of helper RNA generated from pDH(26S) plasmid (Bredenbeek et al., 1993) in BHK-21 cells. Supernatant was collected at 24 hr post-electroporation and concentrated by ultracentrifugation as previously described.

FHV and DCV stocks were prepared on low-passage S2 cells and titers were measured by end-point dilution. S2 cells (2.5×10^5 cells per well in a 96-well plate) were inoculated with 10-fold dilution of virus stocks. At 7 and 14 dpi, the cytopathic effect was analyzed. Titers were calculated as $TCID_{50}$/mL according to a published method (Reed and Muench, 1938).

Human Blood and Ethics Statement

Human blood used in this study was obtained through the ICAReB biobank (https://research.pasteur.fr/en/team/biobanking-icareb/) and manipulated under authorization number HS 2016-24321.

METHOD DETAILS

Isolation of Circular vDNA and Detection by PCR

Fruit flies were injected with 100 $TCID_{50}$ of FHV or 80 $TCID_{50}$ of DCV and collected at 7 days post-infection. Alternatively, fruit flies were injected with 400 PFU of Sindbis-WT or Sindbis-WT+D_G and collected at the indicated time point. *Aedes* mosquitoes were fed 10^5 PFU of the indicated CHIKV stock and collected two weeks post-infection. Individual flies or mosquitoes were crushed in 100 μL of squishing buffer (10 mM Tris, pH 7.5, 60 mM NaCl, 10 mM EDTA, 200mg/μL proteinase K from Eurobiol) and the sample was incubated at 37°C for 1 hr. After phenol-chlorophorm purification, sample was treated for 30 minutes with 50 μg/μL RNase A, then DNA was phenol-chlorophormed again. Finally, 2 μg of resulting DNA was treated with Plasmid-Safe ATP-dependent DNase (Epicenter) for 16 hr at 37°C. ATP and enzyme were added again and the sample was incubated at 37°C for 24 hr. This last step was repeated one time with addition of ATP and enzyme. Enzyme was heat-inactivated 15 minutes at 70°C, before PCR on Rp49 served as a positive control for digestion of linear DNA.

PCR were performed using Phusion polymerase (Thermo Scientitic) according to the manufacturers instruction, using primers 414F and 913R for Sindbis DNA. Primers sequences can be found in the Key Resources Table or in Table S3, related to Figure 1. FHV RNA1 DNA was detected with 69F and 1002R, FHV RNA2 with 70F and 701R, DCV vDNA with 3133F and 4328R or with 4235F and 4863R. Fly linear DNA was detected by targeting Rp49 using primer 144F and 465R. Mitochondrial fly DNA was detected using 794F and 1137R. To detect Sindbis D_G vDNA, primers 1644F and 11041R were used; 1644F and 10656R for D_G cvDNA. cvDNA

detected after Sindbis-replicon injection was detected by nested PCR: a first PCR was performed using primers 91F and 1267R. 0.4 μL of the PCR product was amplified in a subsequent PCR using primers 414F and 913R.

Fly Injection with cvDNA and Survival

S2 cells were infected with 1 MOI of FHV, or not infected, and collected 7 days post-infection. cvDNA was isolated as described in "Isolation of circular vDNA and detection by PCR." To verify the absence of viral RNA, cvDNA stock was reverse transcribed using the Maxima H Minus First Strand cDNA synthesis kit (Thermofisher Scientific) and assessed by PCR.

For immunization, 4-5 days old flies were injected intrathoracically with 10 ng of cvDNA isolated from FHV-infected or non-infected S2 cells. 48 hr later, flies were challenged with 80 $TCID_{50}$ of FHV, 100 $TCID_{50}$ of DCV or control injection (Tris), in 50 nL using a Nanoject II injector (Drummond Scientific). Survival was monitored daily.

Deep-sequencing of Circular vDNA

For generation of FHV cvDNA libraries, S2 cells were infected with 1 MOI of FHV, or not infected, and collected 7 days post-infection. Samples were phenol-chlorophorm purified and processed as described (Lanciano et al., 2017). Briefly, after cvDNA purification using Plasmide-Safe DNase, samples were ethanol-precipitated and amplified by random RCA (Illustra TempliPhi kit, GE Healthcare). DNA concentration was measured with DNA PicoGreen reagent (Invitrogen) and samples were diluted to 0.2 ng/μl. One ng of DNA was used to prepare libraries with the Nextera XT library kit (Illumina). A PCR of 12 cycles was performed with index primers to amplify libraries, before DNA analysis on a high sensitivity DNA Bioanalyzer chip (Agilent Technologies). 2 × 250 nucleotides paired-end sequencing was performed on a MiSeq sequencer (Illumina). Reads were analyzed with in-house Perl scripts

Fly Injection with cvDNA and Deep-sequencing of siRNAs

FHV cvDNA was obtained as described in "Isolation of circular vDNA and detection by PCR ". 4-5 days old flies were injected with 10 ng of FHV cvDNA and collected 3 days post-injection. RNA from 15 flies was extracted using TRIzol reagent (Thermo Fisher Scientific) and processed for next-generation sequencing of small RNAs.

cvDNA Cloning

The overall strategy to clone unintegrated cvDNAs was to linearize isolated cvDNA by digestion with a single-cutter restriction endonuclease and insertion of the linearized cvDNA into a similarly restricted low-copy plasmid vector, pgL338-30, which is commonly used for cloning lentivirus sequences (Cunningham et al., 1993). Restriction endonucleases were chosen based in part on FHV-retrotransponson chimeras identified in Goic et al. (2013). cvDNA was isolated as described above, and digested with either *Sph*1 or *Mlu*1, which cut FHV RNA1 at nt 1036 and 1224, respectively. Following digestion, DNA was isolated and amplified with FHV RNA 1-specific primers containing the *Sph*1 or *Mlu*1 restriction site (Table S2, related to Figure 3). Amplified DNA was isolated, digested with *Sph*1 or *Mlu*1, and ligated to similarly restricted pLg338-30 plasmid DNA. Ligated DNA was used to transform MAX Efficiency Stbl2 Competent Cells (Invitrogen) using procedures recommended by the manufacturer. Colonies were screened by PCR using FHV RNA 1-specific primers and positive colonies were Sanger sequenced using primers specific for FHV RNA 1, pLG338-30 and *Drosophila* retrotransposons (Table S1, related to Figure 4). Sequences were assembled and analyzed using MacVector.

Production of the Sindbis-WT+D_G and Control Stocks

To produce Sindbis-WT+D_G stock, BHK-21 cells were electroporated with 5 μg of Sindbis-WT RNA and 5 μg of D_G RNA in an XCell Gene Pulser Biorad. After 48h, supernatant was collected and concentrated by ultracentrifugation as described.

To produce the Sindbis-WT control stock, a "fake" *in vitro* transcription of D_G RNA was performed, where all the reagents were present except the SP6 enzyme. BHK-21 cells were electroporated with 5 μg of Sindbis-WT RNA and the equivalent in volume of "fake" *in vitro* transcription. In this way, putative traces of D_G plasmid used to produce D_G RNA by *in vitro* trancription were present both in the Sindbis-WT and the Sindbis-WT+D_G stock.

Injection and Titration of Sindbis-Infected Flies

Four to six-days old female flies were intrathoracically injected with 50 nL containing 400 PFU of Sindbis-WT, Sindbis-highDG or Sindbis-equalDG diluted in 10 mM Tris-HCl (pH 7.5). Sindbis-infected flies were frozen at the appropriate time point, crushed in 55 μL of PBS using a Pellet Pestle (Sigma-Aldrich), centrifuged at 10 000 x *g* for 5 min and titrated by plaque assay on Vero cells.

Survival of Sindbis-Infected Flies

Four to six-days old female flies were intrathoracically injected with 50 nL containing 400 PFU of Sindbis-WT, Sindbis-highDG or Sindbis-equalDG diluted in 10 mM Tris-HCl (pH 7.5), or mock-infected with Tris. Survival was monitored daily, and flies were placed on fresh medium every two to three days.

Mosquitoes Rearing, Feeding and Titration

The insectary conditions for mosquito maintenance were 28°C, 70% relative humidity and a 12 h light: 12 h dark cycle. Adults were maintained with permanent access to 10% sucrose solution.

6-8 days old female mosquitoes were fed with 10^5 PFU of CHIKV diluted in prewashed human blood (iCareB platform, Institut Pasteur). Mosquitoes were offered the infectious or control blood meal for 30 min through a membrane feeding system (Hemotek Ltd) set at 37°C with a piece of desalted pig intestine as the membrane. Following the blood meal, fully engorged females were selected and incubated at 28°C, 70% relative humidity and under a 12 h light: 12 h dark cycle with permanent access to 10% sucrose.

Individual mosquitoes were crushed in 70 μL of PBS with a Pellet Pestle (Sigma-Aldrich) and titered by plaque assay on Vero cells. The technique allowed us to detect titers superior to 100 pfu.

AZT Treatment

Wild-type flies were fed daily with 93 mM AZT (Sigma-Aldrich) in 25% sucrose for a week or fed only with sucrose. After a week, flies were infected with 400 PFU of Sindbis or Tris-HCl 10 mM, pH 7.5 (as a control), in 50 nL using a Nanoject II injector (Drummond Scientific).

After infection, flies were kept with a 25% sucrose solution supplemented or not with 93 mM AZT during 3 days. Mosquitoes were fed with a solution of 10% sucrose supplemented with 5 mM AZT a week prior infection and fed with a blood meal as previously described.

Sindbis vDNA Detection by qPCR

vDNA detection by qPCR was performed by injecting 4 to 6-day-old female with 10 000 PFU of Sindbis virus and by freezing the flies at the indicated time point. vDNA was extracted from flies as previously described. qPCR was performed using Power SYBR Master Mix (Applied Biosystems) according to the manufacturer's instruction, and run on a StepOne Plus real-time PCR system machine (Applied Biosystems). Primers 1215F and 1267R were used for Sindbis DNA and primers 144F and 465R were used for Rp49 (Table S3, related to Figures 5 and 7).

Plot of Relative vDNA Production Over Relative Viral Load (Figure 6B)

Relative vDNA Production (y Axis)

Wild-type flies, or the indicated Dcr-2 mutant, where infected with 10 000 PFU of Sindbis-WT or Sindbis-highDG, and vDNA accumulation was measured by qPCR at 7 hr post-infection. Relative vDNA production is calculated by dividing the vDNA production of each fly strain by the value obtained for wild-type flies (mean of 3 independent experiments).

Relative Viral Load (x Axis)

Wild-type or Dcr-2 mutant flies were infected with 400 PFU of Sindbis-WT or Sindbis-highDG, and titers were measured by plaque assay at 3, 5 and 7 days post-infection (n = 10 flies per condition). The percentage of Sindbis-highDG titer relative to Sindbis-WT titer was calculated for these time points. This value was averaged on 3 independent experiments. The final value was obtained by calculating the ratio over the value obtained for wild-type flies.

RNase and DNase Treatments

DNA extracted from individual flies was digested with 10 μg/mL of RNase A/T1 (Thermo Fisher Scientific) 1 hr at 37°C, then phenol-chlorophorm-purified. Alternatively, DNA was digested using the Turbo DNA-free kit (Life technologies) according to the manufacturers' instructions. vDNA was measured by qPCR.

DVGseq Pipeline

Individual flies were crushed in 1 mL of TRIzol reagent (Invitrogen) using a Pellet Pestle (Sigma-Aldrich) and RNA was extracted following the manufacturer's instructions. cDNA was produced using 100 ng of RNA using the Maxima H Minus First Strand cDNA synthesis kit (Thermo Fisher Scientific) according to the manufacturer's instructions. cDNA was further amplified by PCR using Phusion polymerase using the primers 414F and 11634R for Sindbis (Table S3, related to Figure S2). PCR products were purified on NucleoSpin Gel and PCR Clean-up column (Macherey-Nagel). For every analysis, RNA was extracted in bulk. Reverse-transcription, as well as PCRs, were performed in the same 96-well plate. For controls, *in vitro* transcribed RNA of the virus of interest was included, mixed or not with different amount *in vitro* transcribed RNAs of known DVG. Because every step of the pipeline is performed in bulk, DVG detected in samples that are artifacts (for example artifacts of PCR) can be removed because they will be present in the controls. PCR products were fragmented (Fragmentase, Thermo Fisher Scientific) before their linkage to Illumina multiplex adapters, their clusterization and sequencing (Illumina cBot and GAIIX technology). CASAVA software was used to demultiplex the sequences. The sequenced reads for each sample were aligned to their respective reference genomes using BWA MEM. Samples with < 100,000 aligned reads were excluded from further analysis. DVG reads were identified as chimeric reads (identified with SA tags) consisting of two linear alignments covering the whole read. The end position of the leftmost alignment and the start position of the rightmost alignment were referred to as ''cut start position'' and ''cut end position,'' respectively. DVG were defined as a set of > 100 DVG reads with the same cut start and end positions. DVG with cut start position < 600 were found in control samples containing only full-length viral RNA; we consequently concluded they were due to PCR artifacts and removed them from further analyses

in all samples. The raw frequency of a DVG was computed from the drop in number of reads before and after the cut start or end position (chosen so as to increase power):

$$f_r = \frac{N_i - N_{i+1}}{N_i} \text{ if } N_i > N_j; \quad f_r = \frac{N_j - N_{j-1}}{N_j} \text{ otherwise,}$$

where f_r denotes the raw frequency, N_k the total number of reads at position k, i the cut start position, j the cut end position and L the genome length. Because of PCR biases toward amplifying DVG rather than full-length genomes, raw frequencies were overestimating DVG frequencies, and we used control samples containing mixes of full-length and D_G RNA at different ratios to normalize these frequencies in each individual plate. Raw frequencies were linked to actual frequencies by the following equation:

$$\log\left(\frac{f_a}{1-f_a}\right) = \alpha \log\left(\frac{f_r}{1-f_r}\right) + \beta,$$

where f_r denotes raw frequencies and f_a denotes actual frequencies; α and β are fixed parameters. One such linear regression was fitted per plate, using the control samples (all adjusted R^2 were > 0.98), and was used to normalize raw frequencies of DVG.

Deep-sequencing of Small RNAs

WT, *Dcr-2*^{G31R}, *Dcr-2*^{A500V} or *Dcr-2*^{L811fX} were injected with 400 pfu of Sindbis-WT and collected at 7 days post-infection; RNA was extracted from 15 flies using TRIzol and processed for small RNAs sequencing. 19-29 nt RNAs were purified from a 15% acrylamide/bisacrylamide (37.5:1), 7 M urea gel and used for library preparation using NEBNext Multiplex Small RNA Library Prep (Illumina, New England Biolabs). The 3′ adaptor from Integrated DNA Technologies (linker 1) and in-house-designed indexed primers were used in the process. Sequencing of librairies diluted to 4 nM was performed on a NextSeq 500 sequencer (Illumina) with a NextSeq 500 High-Output Kit v2 (Illumina) (75 cycles). Reads were analyzed with in-house Perl scripts. Graphs were generated with FastQC (www.bioinformatics.babraham.ac.uk/projects/fastqc/) to assess the quality of fastq files. Adaptors and low-quality bases were trimmed from reads using cutadapt (https://cutadapt.readthedocs.io/en/stable/) and reads with low quality were eliminated. Reads were mapped on genomes using bowtie1 (Langmead et al., 2009) to generate sam files, allowing one mismatch between a read and its target. Sam files were processed to produced bam indexed files using samtools package (Li et al., 2009). Graphs were generated from bam files using in-house R scripts and the Bioconductor Rsamtools and Shortreads libraires (Morgan and Grimshaw, 2009).

Construction of Dcr-2 helicase Expression Plasmid

The helicase domain of Dcr-2 was cloned as a V5/3XFLAG tagged fusion protein into pAc 5.1 V5 His(A) (Invitrogen) using the restriction free cloning method. The 3XFLAG region from p3XFLAG-CMV-9 Expression Vector (Sigma-Aldrich) was amplified by PCR using primers Flag_F and Flag_R (Table S3, related to Figure 6). This PCR product was used as a primer for a second PCR using pAc 5.1 V5 His(A) as template. During this amplification step, the His tag was removed from the original plasmid. To clone the helicase of *Drosophila melanogaster* Dcr-2 in pAc 5.1 V5 3XFLAG, Dcr-2 helicase was amplified by PCR from cDNA from wild-type flies (w^{1118}) with primers Dicer-2_Flag_F and Dicer-2_Flag_R (Table S3, related to Figure 6). The purified PCR product was used as primer for a PCR using pAc 5.1 V5 3XFLAG as a template. The resulting plasmid, designated *pAc5.1 Dcr-2 helicase V5 3XFLAG*, carries the coding region of Dcr-2 helicase downstream of the *Drosophila* actin promoter and two tags for protein purification in the C-terminal region, V5 and 3XFLAG. Final plasmid was sequenced to verify the presence of inserts at the desired positions without mutations, deletions or insertions.

Immunoprecipitation Assays

S2 cells were seeded at 1x 10^6 cells in 6 wells plate and transfected with 400 ng/well of *pAc5.1 Dcr-2 helicase V5 3XFLAG* using Effectene Transfection Reagent (QIAGEN) following manufacturer's indications. Controls included empty vector *pAc5.1 V5 3XFLAG* and *pAc5.1 CG4572 V5 3XFLAG.* The next day, cells were extensively washed and infected with Sindbis highDG or Sindbis wt (MOI = 2,5). At 72 h post-infection, cells were collected and 10% was kept for RNA extraction with TRIzol (designated input RNA). The remaining cells were homogenized in 100 uL of cold lysis buffer containing 50 mM Tris pH 7.5, 150 mM NaCl, 2.5 mM MgCl2, 250mM sucrose, 0.05% NP-40, 0.5% Triton X-100, 10% glycerol, 1mM DTT, 1mM EDTA, 1X protease inhibitor cocktail (Roche), 5uL/mL RNase OUT (Thermo Fisher Scientific) and incubated for 30 minutes at 4°C with rocking agitation. Cell lysates were clarified by centrifugation at 12,000 rpm for 15 minutes (4°C), and protein concentration in the supernatant was determined using the Bicinchoninic Acid Assay (Pierce). For immunoprecipitation, 100 mg of total lysate were incubated in a final volume of 1 mL lysis buffer with either 9 ug pre-equilibrated ANTI-FLAG M2 Magnetic Beads (Sigma) or Gammabind Plus Sepharose (GE Healthcare) coupled with 10 ug V5 monoclonal antibody (Invitrogen). Reactions were incubated using a roller shaker for 4 h at 4°C, washed 3X in TBS buffer (50 mM Tris pH 7.5, 150 mM NaCl) supplemented with 250mM sucrose and 0.5mM DTT followed by a final wash in TBS supplemented with 250mM sucrose and 0.5mM DTT and RNase OUT. Samples were eluted either with 3X Flag Peptide (Sigma) or lysis buffer without protease inhibitors at high stringency conditions (800mM NaCl) with proteinase K treatment. Eluates were then further subjected to RNA isolation (TRIzol) and RT-PCR for detection of Sindbis virus RNA.

QUANTIFICATION AND STATISTICAL ANALYSIS

The (non-parametric) log-rank test was used to compare survival curves (Figures 1F, 1G, 7B, 7D, and S5B–S5D). Two-way ANOVA was performed to compare viral titers of two viruses over time (Figures 5C, 5D, S2C–S2F, S4A, and S4B) following log-transformation; homoscedasticity and normality of the distributions were satisfactory, and treatment (virus) effect was reported. To compare two distributions, the non-parametric Mann–Whitney test was used (Figures 5E, 7A, 7C, S2B, S3A, S3C, and S5A). To compare mosquito outcome (infected or not) between different viruses, we performed χ^2 tests of independence on 2 × 2 contingency tables (Figures 5F and 5G). All statistical tests were performed on Graphpad Prism version 5 (https://www.graphpad.com/). *P*-values < 0.05 were considered significant.

DATA AND SOFTWARE AVAILABILITY

The accession numbers for the RNA, DNA, and small RNA sequences reported in this paper are SRA NCBI: PRJNA387403, PRJNA387406, PRJNA416764, and PRJNA416718.